Phosphorus recycling in photorespiration maintains high photosynthetic capacity in woody species

Phosphorus recycling in photorespiration maintains high photosynthetic capacity in woody species

DAVID S. ELLSWORTH[1,*], KRISTINE Y. CROUS[1], HANS LAMBERS[2], JULIA COOKE[1,3]

[1] *Hawkesbury Institute for the Environment, Locked Bag 1797, University of Western Sydney, Penrith, NSW, 2751, Australia*

[2] *School of Plant Biology, The University of Western Australia, 35 Stirling Highway, Crawley (Perth), WA 6009, Australia*

[3] *Department of Biological Sciences, Faculty of Science, Macquarie University, North Ryde, NSW 2109, Australia*

[*] *Corresponding author* (D.Ellsworth@.uws.edu.au)

Received: 18th September 2014

Running Head: PHOSPHORUS RECYCLING IN PHOTORESPIRATION

ABSTRACT

Leaf photosynthetic CO_2 responses can provide insight into how major nutrients such as phosphorus (P) constrain leaf CO_2-assimilation rates (A_{net}). However, triose-phosphate limitations are rarely employed in the classic photosynthesis model and it is uncertain to what extent these limitations occur in field situations. In contrast to predictions from biochemical theory of photosynthesis, we found consistent evidence in the field of lower A_{net} in high [CO_2] and low [O_2] than at ambient [O_2]. For ten species of trees and shrubs across a range of soil P availability in Australia, none of them showed a positive response of A_{net} at saturating [CO_2] (i.e. A_{max}) to 2 kPa O_2. Three species showed >20% reductions in A_{max} in low [O_2], a phenomenon explained by orthophosphate (P_i) savings during photorespiration. These species, with largest photosynthetic capacity and P_i > 2 mmol P m^{-2}, rely the most on additional P_i made available from photorespiration rather than species growing in P-impoverished soils. The results suggest that rarely-used adjustments to a biochemical photosynthesis model are useful for predicting A_{max}, and give insight into the biochemical limitations of photosynthesis rates at a range of leaf P concentrations. Phosphate limitations to photosynthetic capacity are likely more common in the field than previously considered.

INTRODUCTION

The net CO_2-assimilation rate (A_{net}) of C_3 leaves in sunlight comprises three principal processes occurring at the same time: photosynthesis, photorespiration and mitochondrial respiration in the light. A major theoretical advance in the ability to understand and model leaf and canopy CO_2 exchange incorporating elements of all three processes was afforded by the biochemical model of photosynthesis of Farquhar *et al.* (1980), further described in von Caemmerer (2000). This model, originally formulated by Farquhar *et al.* (1980) (here termed the FvCB model) allows for inferences to be made about biochemical limitations to leaf and canopy functioning, overlain by environmental constraints (Long & Bernacchi 2003). The original FvCB model (Farquhar *et al.* 1980) and its subsequent modifications (Sharkey 1985; Sharkey *et al.* 2007; von Caemmerer 2000) successfully predicts photosynthesis under a very wide range of conditions, and has been applied to scales ranging from the chloroplast (von Caemmerer 2013) to forest canopies (Groenendijk *et al.* 2011) and biomes (Bonan *et al.* 2011; Kattge *et al.* 2009). A unique element of the FvCB model is the ability to estimate photorespiratory CO_2 efflux concurrent with photosynthetic CO_2 influx as component processes contributing to the net CO_2-assimilation rate of leaves (Busch 2013; Sage & Sharkey 1987). Both component processes need to be considered to predict net CO_2 assimilation as they occur at the same time, and together have implications for predicting the response of leaf CO_2 assimilation to rising atmospheric CO_2 concentrations, given that elevated [CO_2] both stimulates photosynthesis and suppresses photorespiration (Sharkey 1988; von Caemmerer 2000).

The FvCB biochemical model of photosynthesis has provided a useful context for interpreting many mechanistic aspects of plant function, including how the availability of major nutrients to plant canopies can restrict photosynthetic capacity and net primary productivity (Kattge *et al.* 2009). Analyses of nitrogen (N) limitations to photosynthetic capacity have been based on the fact that a major fraction of leaf N is allocated to the Rubisco enzyme (Evans 1989). The large proportion of leaf N invested in Rubisco and related photosynthetic proteins means that two major parameters of the FBvC model, the maximum carboxylation rate (V_{cmax}) and the capacity for electron transport to support RuBP regeneration (J_{max}), tend to scale linearly with leaf [N] in herbaceous crop species (Archontoulis *et al.* 2012; Evans 1989) and in woody species (Ellsworth *et al.* 2004; Rogers 2014). Such relationships are now used in a number of

ecosystem and global-scale models to assess ecosystem productivity of N-limited ecosystems (Piao *et al.* 2013; Rogers 2014; Williams *et al.* 1997; Zaehle *et al.* 2014). However, P limitation of plant productivity is also widespread, with up to one-third of the world's soil orders demonstrating low P availability (Yang & Post 2011). In contrast to N, it is less clear how low leaf P concentration in P-limited systems may affect photosynthetic biochemistry. There are suggestions of both direct and indirect roles of P regulating A_{net} (Domingues *et al.* 2010; Pieters *et al.* 2001; Thomas *et al.* 2006). Hence, a mechanistic representation of P limitations to leaf CO_2 assimilation is rarely implemented in either leaf-to-canopy (Bernacchi *et al.* 2013; Long & Bernacchi 2003; Manter & Kerrigan 2004) or large-scale models (Wang *et al.* 2010), despite the importance of P as a major limiting element across tropical, subtropical and some temperate ecosystems (Aerts & Chapin 2000; Lambers *et al.* 2010; Vitousek *et al.* 2010).

Low P supply from soils can affect bulk leaf P concentration and decrease leaf orthophosphate (P_i) pools as well as reduce leaf net CO_2-assimilation rate and other components of photosynthetic biochemistry (Hammond & White 2011; Veneklaas *et al.* 2012). Since P-containing molecules such as ATP, NADPH, and sugar-phosphates including ribulose-1,5-bisphosphate (RuBP) have key roles in the Calvin-Benson cycle, lack of sufficient P and P_i would be expected to limit the maximum light- and CO_2-saturated A_{net} (A_{max}) that can be achieved in leaves (Brooks 1986; Loustau *et al.* 1999). Such a decrease in the concentration of these metabolites upon P starvation is typical for plants that are not adapted to P-impoverished soils. Conversely, Proteaceae from severely P-impoverished soils in Australia do not operate at lower leaf P metabolite concentrations at very low soil P availability, but rather replace phospholipids by galactolipids and sulfolipids (Lambers *et al.* 2012) and operate at very low levels of ribosomal RNA and proteins (Sulpice *et al.* 2014). Still, P-limitation might be manifest in limiting RuBP regeneration as the underlying control over A_{max} in leaves (Campbell & Sage 2006; Jacob & Lawlor 1993). Whilst evidence for RuBP regeneration limitation by low P_i exists in laboratory studies (Jacob & Lawlor 1993), the mechanism by which low leaf [P] decreases photosynthetic capacity is not well defined and field evidence of such limitations is still lacking.

One approach for quantifying P-limitations to the biochemistry of net CO_2 assimilation is by estimating triose-P limitations following theory proposed by Sharkey (1985). The basis of this theory is that RuBP regeneration is adenylate-limited, and a

release from this limitation is achieved by the release of P_i associated with precursors for sucrose synthesis in the cytosol. Exchange of each released P_i for triose-P produced in the chloroplast allows continued triose-P export to the cytosol (Paul & Foyer 2001; Stitt *et al.* 2010; see A in Fig. 1). An alternative hypothesis is that triose-P limitation is related to how 'closed' the photorespiratory cycle is with regard to the return of glycerate to the chloroplast via photorespiratory glycolate metabolism in the peroxisomes and mitochondria (Harley & Sharkey 1991; Fig. 1, highlighted as B). Short-term low-photorespiratory conditions using low O_2 partial pressure in air (pO_2) can be used as a probe of these biochemical limitation mechanisms to A_{net}. However, whilst triose-P limitations are often mentioned in publications describing the FBvC photosynthesis model, they are rarely parameterised (Bernacchi *et al.* 2013; Manter & Kerrigan 2004), except in very few studies where plants are grown at very low P supply (Bown *et al.* 2009; Domingues *et al.* 2010; Loustau *et al.* 1999).

To investigate P limitations to photosynthetic capacity in the field, we sought to determine if these limitations have a role in regulating the biochemical processes underlying leaf A_{net} in the field. We specifically asked *i*) if the standard two-limitation version of the FvCB model (Farquhar *et al.* 1980; Farquhar *et al.* 2001) is adequate to characterise the major parameters controlling photosynthetic capacity for species growing at a range of leaf P and P_i concentrations, *ii*) is there evidence of triose-P limitations to A_{net} using non-photorespiratory gas exchange analysis, and *iii*) are triose-P-utilisation limitations to A_{net} associated with concentrations of bulk leaf P or P_i? Our null hypothesis was that leaf photosynthetic capacity at both normal (ambient pO_2 of 21 kPa) and low pO_2 could be described adequately by the two-limitation version of the FvCB model. In this study we used the tool of providing nearly non-photorespiratory conditions by measurements under low pO_2 to gain insight into the processes regulating leaf A_{net}. This was done for Australian sclerophyll plants at a range of leaf P levels in both eastern and south-western Australia, including locations characterised by some of the lowest soil P availabilities on earth (Lambers *et al.* 2010) as well as sites with moderate P availability. In so doing, we sought to resolve whether plants with low leaf P were more likely to show triose-P limitations than those at higher leaf P levels, an idea that is occasionally cited (see Domingues *et al.* 2010; Loustau *et al.* 1999). We chose a set of native species that included species of *Eucalyptus* and *Acacia* and species in the

Proteaceae as three groups dominating the Australian continent, and *Liquidambar styraciflua* L. which is not native to Australia or similarly low-P soils.

METHODS AND THEORIES

Theory from the Farquhar et al. *(1980) photosynthesis model*

Analysis of the instantaneous response of leaf net photosynthesis to brief changes in the CO_2 concentration surrounding leaves underpins the FBvC model parameterisation (Long & Bernacchi 2003; von Caemmerer 2000). According to the standard FvCB model based on the stoichiometry of carbon in photosynthesis and photorespiration (Farquhar *et al.* 1980; von Caemmerer 2000), the net CO_2-assimilation rate of a leaf (A_{net}) can be expressed as

$$A_{net} = v_c - 0.5v_o - R_d = v_c\left(1 - \Gamma^*/C_i\right) - R_d \quad (1)$$

with v_c and v_o denoting the carboxylation and oxygenation rates of the Rubisco enzyme, R_d representing the rate of mitochondrial respiration in the light, Γ^* representing the CO_2 concentration at which the photorespiratory efflux of CO_2 equals the rate of photosynthetic CO_2 uptake, and C_i indicating the internal CO_2 concentration in the substomatal cavity. As there is also a liquid-phase resistance between the intercellular surfaces and the sites of carboxylation in the thylakoids, this equation is best expressed using C_c, the chloroplastic CO_2 concentration, rather than C_i thus incorporating mesophyll conductance to CO_2 transfer in the liquid phase (Pons *et al.* 2009). Thus, carboxylation rate and hence A_{net} is limited by one of two rates, W_c and W_j (Farquhar *et al.* 1980), later revised to include a third rate-limiting process W_t (Sharkey 1985):

$$v_c = \min\{W_c, W_j, W_t\} \quad (2)$$

W_c is the carboxylation-limited rate of net CO_2 assimilation when chloroplastic RuBP is saturating, W_j is the energy transduction for ATP synthesis leading to the subsequent regeneration of ribulose 1,5-bisphosphate (RuBP) in the photosynthetic carbon-reduction cycle, and W_t is the net CO_2-assimilation rate when triose-P pools tie up the available orthophosphate (P_i) for synthesising ATP needed in the photosynthetic carbon reduction or Calvin-Benson cycle (Bernacchi *et al.* 2013; Sharkey *et al.* 2007).

When Rubisco activity limits photosynthetic CO_2 assimilation (W_c), A_{net} is given by

$$A_{net} = V_{cmax}\frac{C_c - \Gamma^*}{(C_c + K')} - R_d \quad (3)$$

where the half-saturation constant $K' = k_c\left(1 + O_i / k_o\right)$. Here V_{cmax} is the maximum catalytic activity of Rubisco with saturating RuBP, C_c and O_i are the chloroplastic CO_2 and intercellular O_2 gas partial pressures, respectively, and k_c and k_o are the Michaelis-Menten coefficients of Rubisco for CO_2 and O_2 (see Bernacchi *et al.* 2013; Sharkey *et al.* 2007). The photosynthetic CO_2-compensation point (Γ^*) is the CO_2 concentration at which the photorespiratory efflux of CO_2 equals the rate of photosynthetic CO_2 assimilation. Given that the Rubisco enzyme is characterised by relatively conservative kinetic properties among different lineages of higher C_3 plant species, k_c, k_o and Γ^* can be assumed as relatively invariant among species (Bernacchi *et al.* 2001; but see Galmés *et al.* 2005; Walker *et al.* 2013). In the classic version of the FvCB model, when C_c is close to saturation for photosynthesis such that RuBP regeneration limits photosynthesis (W_j is limiting), A_{net} is given by

$$A_{net} = J_{max}\frac{C_c - \Gamma^*}{(4C_c + 8\Gamma^*)} - R_d \quad (4)$$

where J_{max} is the maximum rate of electron transport at saturating quantum flux density to provide energy for RuBP regeneration in the PCR cycle. Most frequently, the parameters V_{cmax} and J_{max} are investigated as the major components of the photosynthesis model (Cernusak *et al.* 2011; Kattge *et al.* 2009; Rogers 2014; Walker *et al.* 2014) assuming two major biochemical limitations to A_{net}. However, as originally stated, the FvCB photosynthesis model has no explicit dependence of J_{max} on O_2 partial pressure except Γ^* in Eqn 4. The Γ^* term is a function of the *in vivo* substrate specificity factor for the Rubisco enzyme ($S_{c/o}$), given as:

$$\Gamma^* = \frac{0.5 \cdot O}{S_{c/o}} \quad (5)$$

Where $S_{c/o}$ is here considered ≈ 92 mol mol^{-1} at 25°C, within the range reported for C_3 woody species (Galmés *et al.* 2005). The original version of the FvCB photosynthesis model produces predictions of the A_{net}-C_c response at normal air pO_2 (21 kPa, hereafter referred to as normal pO_2) and low-photorespiratory pO_2 that are illustrated in Fig. 2 (see also von Caemmerer 2000).

FvCB photosynthesis model with triose-phosphate limitation included

Two modifications of the original FvCB model were subsequently proposed to account for the behaviour of A_{net} measured at high CO_2 partial pressures and with suppression of photorespiration at experimentally reduced O_2 partial pressures. These changes to the model accounted for two physiological states that have been observed both at high CO_2 partial pressures: *i*) O_2 insensitivity of A_{net} at high pCO_2, and *ii*) reverse O_2 sensitivity of A_{net}. In the first version, synthesis of sucrose from triose-phosphates was thought to make a contribution to P_i recycling for photophosphorylation since the triose-P transporter exchanges triose-P for P_i. For the situation when the rate at which triose phosphates are utilised (T_p) in the synthesis of carbohydrates limits A_{net} (W_t in Eqn 2), Sharkey (1985) proposed that

$$A_{net} = 3 \cdot T_p - R_d \qquad (6)$$

As there is no term dependent on pO_2 in Eqn 6, there is no explicit sensitivity to low pO_2 in this variant of the model. It was found that this model version might not always account for leaf gas exchange behaviour in low pO_2 (Harley & Sharkey 1991; Sage & Sharkey 1987), promoting an updated version of the model formulation.

In this updated version, Harley & Sharkey (1991) further proposed consideration of the pO_2 sensitivity of light- and CO_2-saturated net CO_2-assimilation capacity (A_{max}) through an 'open' photorespiratory C cycle. This version of the FvCB model has a pO_2 sensitivity that originates indirectly from ATP consumed with metabolism of the photorespiratory product, glycolate, in the chloroplast (α_g) (Fig. 1, B) as given by

$$A_p = \frac{\left(C_c - \Gamma^*\right) \cdot 3T_p}{C_c - \left(1 + 3 \cdot \alpha_g\right) \cdot \Gamma^*} - R_d \qquad (7)$$

The parameter α_g is multiplied by three to reflect the stoichiometry of P_i consumption in oxygenation (von Caemmerer 2000; note the correct version of the equation here), and varies as a fraction between 0 and 1 depending on whether all glycolate returns to the chloroplast (a 'closed' photorespiratory cycle where C is maximally conserved, in which case Eqn 7 simplifies to Eqn 6), the return is partial, or glycolate is entirely diverted to amino acid synthesis leaving none to return (Harley & Sharkey 1991).

More than 20 years after it was proposed, this third term of the model (Eqns 6 and 7) is rarely considered in photosynthesis model fits to data (von Caemmerer 2013) and most often ignored (Kattge *et al.* 2009; Manter & Kerrigan 2004; Walker *et al.*

2014). This is due in part to a lack of appropriate measurements (Long & Bernacchi 2003; von Caemmerer 2000) and because the evidence supporting its importance in leaves with low P concentration has been equivocal (Domingues *et al.* 2010). Moreover, T_p has almost never been parameterised in field situations, so it remains unclear if this term needs to be considered in modelling limitations to photosynthetic CO_2 assimilation (Bernacchi *et al.* 2013). If T_p can largely be ignored, we expect a stimulation of A_{net} by low pO_2 in all parts of the CO_2-response curve as per Figure 2. Our field measurements of plants at high and low leaf P status aimed to understand if the mechanistic hypotheses of triose-P limitations to photosynthesis portrayed in Eqns 6 and 7 are consistent with field data, and if these revisions can reflect the role of P availability for regulating A_{net}. If there is an association between plant P status and T_p, then incorporation of this parameter into models may improve the predictability of A_{net}, especially where rising atmospheric CO_2 concentration and low soil P availability are concerned.

Research sites and plant material

The research was conducted on trees and shrubs growing at five different sites in eastern and south-western Australia (Table 1), with different soil substrates and parent materials resulting in different leaf P content in their characteristic species. Sites were chosen based on known aspects of their mineralogy and previous studies on leaf nutrients (e.g., Lambers *et al.* 2012) so that they would provide a range in leaf total P and P_i fraction and thus presumably represent a range in P_i limitations to A_{net}. Four of the five sites were infertile and low in P availability, with the fifth site on a richer soil. The Davies Park site is located at 390 m above sea level (a.s.l.) in the Blue Mountains in eastern Australia on thin soils overlaying Hawkesbury sandstone, a Triassic sedimentary quartzose sandstone formed over 200 Mya. The soils derived from the Hawkesbury sandstone in the Blue Mountains are shallow (5-20 cm depth) and very infertile with low P availability. The Hawkesbury Forest Experiment and adjacent Hawkesbury campus and EucFACE sites are all located at 30 m a.s.l. within 1 km of one another on Clarendon loamy sand, a deep, alluvial soil formed in the late Pleistocene by meanders of the Hawkesbury river around 1.5 Mya. The soil is a low-fertility loamy sand, with soil surface total P concentrations of 60 mg kg^{-1} soil in the upper 15 cm (Ellsworth *et al*., unpubl. data), but a large fraction of this P is sorbed onto

aluminosilicates and ferro-manganesian silicates (Holford 1997). One of the plantations at this site (*Liquidambar styraciflua* L.) was horticulturally managed and had periodically-amended soil P. The Lesueur National Park site is described in detail in (Lambers *et al.* 2012). This site is located near Jurien Bay, WA and occurs at 80 m a.s.l. on shallow colluvial sand and lateritic gravel over weathered sandstone from the late Jurassic Yarragadee Formation (150-185 million years old; Griffin & Burbidge 1990). The sandy soil at this site is extremely low in P, with a total P of 9.5 mg kg^{-1} soil in the upper 30 cm (Lambers *et al.* 2012). The fifth site, Illawarra Fly in Robertson NSW, is a fertile site on young soils. This site occurs at 710 m a.s.l. elevation on soils of the Illawarra escarpment that are brown clay loams underlain by Paleocene/Pliocene basalt. These basaltic soils in the area are relatively fertile with total P of 1010 mg kg^{-1} soil and frequently managed for farming, though this particular site was in a never-farmed parcel of mature remnant wet sclerophyll forest. Since sites differed in elevation, amounts of gases such as CO_2 and O_2 are reported as partial pressures (e.g., pO_2) rather than mole fractions.

Whilst the focus was on measuring species of *Eucalyptus* as native dominants in the study regions, non-Myrtaceous species were also included (*Banksia* spp. and *Persoonia levis*, all Proteaceae, and *Acacia oblongifolia*). An exotic deciduous plantation tree, *Liquidambar styraciflua*, was also included in the study so that inferences would not be strictly limited to native Australian sclerophyll species, which are considered to be well-adapted to low soil P (Beadle 1966).

CO_2-exchange measurements

In this study, photosynthetic CO_2-response curves (A_{net} - C_i response curves) were made *in situ* on ten species of trees and shrubs at five sites in Australia (Table 1) using a portable photosynthesis system (LiCor 6400XT, Licor Inc., Nebraska USA) with 6 cm^2 chamber. All measurements were made on attached, intact leaves at the top of the crown or the outer shell of the crown when open-grown which meant accessing leaves from 1 m up to 25 m high (Table 1). For tall species, access to the upper parts of the tree crowns was achieved by three different means: an articulated boom lift (Snorkel MHP13/35 Trailer Mounted Lift, Snorkel Ltd., Meadowbrook, Qld, Australia) used at the Hawkesbury site in Richmond NSW, a set of 36 m tall construction cranes (Jaso crane J-4010, Jaso S.L., Idiazabal, Spain) at the nearby EucFACE site in Richmond NSW, and a

custom-built steel-alloy canopy walkway going up from ground level to 30 m height ('Illawarra fly') at Robertson, NSW. Canopy access was not necessary at the Lesueur National Park site or at Davies Park, as trees and shrubs were open-grown in each of the sclerophyll woodlands, and unshaded leaves at the outside of the crown could be readily measured.

We made field measurements of the instantaneous response of leaf net CO_2 assimilation to changes in the external CO_2 concentration according to Ellsworth *et al.* (2004), using standard coefficients recommended in Sharkey *et al.* (2007) when fitting the FvCB model (see below). A_{net}-C_c response measurements on all species were made during the growing season in summer and autumn at seasonal temperatures and during periods of recent rainfall to reduce complications due to drought. Previous–year's leaves were measured rather than newly-emerged leaves to ensure that leaves were operating at their full photosynthetic capacity (see Denton *et al.* 2007; Lambers *et al.* 2012). The A_{net} measurements were made in morning hours on sunny days so as to avoid stomatal closure and mid-day depression of A_{net}.

The A_{net}-C_c response curves were started by maintaining the CO_2 concentration (C_a) in the gas exchange chamber at ambient CO_2 partial pressure (~38-39 Pa in this study) until gas-exchange rates were stable, then recording measurements. Steps for the curves were generated by decreasing C_a to near the compensation point (5 Pa), and then increasing C_a stepwise across 8-9 steps (Ellsworth *et al.* 2012) at a constant photosynthetic photon flux density of 1800 μmol m^{-2} s^{-1}, 50-70% relative humidity, and a controlled leaf temperature (between 26 and 28°C, depending on species). The mean leaf-air vapour pressure deficit of the measurements was 1.5 ± 0.1 kPa. At each C_a step, we recorded A_{net}, g_s, C_i and associated variables when stability was reached. Upon completion of measurements, leaves were placed on ice or liquid nitrogen until ready for further analysis. In the lab, leaf thickness was measured at five points on the leaf lamina using digital callipers (Mitutoyo Corp, Kawasaki, Kanagawa, Japan).

In the process of these A_{net}-C_c response measurements, at four or five of the C_a steps, we ensured that parallel measurements at ambient oxygen (21 kPa) and low-photorespiratory oxygen (2 kPa) were made. Low pO_2 inside the gas exchange chamber was generated by routing a low-O_2 tank gas (Air Liquide Australia Ltd., Melbourne, Australia) to the leaf chamber, supplied at the same slight over-pressure as for ambient air as described by Li-Cor (Li-Cor 2008) and with the excess flow to the Li-6400 pump

monitored with a rotameter. A Teflon T-valve was toggled between ambient air with 21 kPa pO_2 and 2 kPa tank gas at the appropriate C_a steps (up to five C_a steps including at saturation). These steps were chosen in order to minimally define the initial rise to a maximum and the maximum asymptote for the A_{net}-C_c curve at low pO_2, given that the shape of these curves has long been known (Laing *et al.* 1974; von Caemmerer 2000). The flow excess was maintained around 0.3 L min^{-1}. Measurements of A_{net} in 2 kPa pO_2 were completely reversible as described in Laing *et al.* (1974)(see Supporting Information, Fig. S1).

Calculations of O_2 corrections and mesophyll conductance to CO_2

We used three corrections for changes in pO_2 in the carrier-gas in the LI-6400XT photosynthesis system that originated from the change in density due to different gas concentrations. The corrections employed were: i) increased air-flow rate through the CO_2-injector system due to reduced air viscosity with decreased pO_2 , ii) band broadening of CO_2 infrared absorption (Burch *et al.* 1962) incorporated into the standard Li-6400 software, and iii) band broadening of water vapour infrared absorption (Bunce 2002).

Given theoretical issues raised by Gu & Sun (2014) concerning the dependence of mesophyll conductance to CO_2 (g_m) on C_i, we assumed a constant g_m for different C_i steps in the response-curve data. Mesophyll conductance was either measured or estimated for each species for calculations of C_c. For three species amongst those in Table 1 ranging in A_{net} from highest and lowest, we measured instantaneous g_m with online carbon-isotope discrimination using tunable diode laser absorption spectroscopy (TDLAS; Campbell Scientific TGA100A, Logan, UT, USA). Our g_m calculations follow Tazoe *et al.* (2011) with further description in Crous *et al.* (2013). We then estimated mean g_m of all the species using a relationship for g_m as a function of g_s from our measurements ($g_m = -0.04 + 1.34*g_s$, $r^2 = 0.54$; Supporting Information Fig. S2). In a review of available data, g_m usually scaled with g_s especially amongst well-watered plants (Flexas *et al.* 2012). After incorporating g_m, we derived biochemical model parameters using the A_{net}-C_c data.

Photosynthetic parameter fits were done in R (Team 2014) using kinetic coefficients in Sharkey *et al.* (2007) to standardise the fits across species, but using Γ* and its temperature dependence specifically measured for *Eucalyptus* (Crous *et al.*

2013). We fit V_{cmax}, J_{max} and T_p piece-wise using specified ranges of conditions where each parameter was judged to limit A_{net} following guidelines in Sharkey *et al.* (2007) with the nonlinear solutions generated using the 'optim' package in R. T_p was fit for A_{net} when C_c > 40 Pa and pO_2 of 2 kPa. As a more robust fitting approach with fewer assumptions, we also pooled data for all leaves within a species and simultaneously solved for species-level V_{cmax}, J_{max} and T_p at both pO_2 levels using the 'nls' package in R. Across species, the two sets of solutions agreed well with one another, since slopes for each parameter were close to unity (slopes of 0.981, 0.966 and 0.840 for V_{cmax}, J_{max} and T_p, respectively, estimated for piecewise compared with simultaneously-solved). V_{omax}, the maximum velocity of oxygenase activity, was fit to the data from both pO_2 levels for low C_c where oxygenase activity of Rubisco is considered limiting, following equations in Farquhar *et al.* (1980).

Leaf chemical analyses

After measurements, leaves were immediately placed on ice and transported to the laboratory, where thickness and area were measured on a subsample, whilst the remainder was frozen and subsequently dried to a constant mass at 70 ˚C. The leaf lamina dry mass per unit area (M_a) was calculated from the ratio of dry mass to fresh area. The dried sample was ground finely in a ball mill, and used for analyses of total N concentration, total P concentration, inorganic P (P_i) concentration, and starch and soluble sugar concentrations. Leaf N concentration was analysed by elemental analysis after combustion using a CHN elemental analyser (TruSpec micro, LECO Corp., St. Joseph, MI, USA; or FLASH EA 1112 Series CHN analyser, Thermo-Finnigan, Waltham, MA USA). Leaf total P concentrations were measured after digesting dried leaf tissue with concentrated sulfuric acid (H_2SO_4) and hydrogen peroxide (H_2O_2) in a microwave digester apparatus (Berghof speedwave four, Berghof Products GmbH, Eningen, Germany). The solutions containing total P or the P_i fraction were analysed colourimetrically at 880 nm (AQ2, SEAL Analytical, Ltd., Milwaukee, WI USA) after a standard molybdate reaction (Close & Beadle 2004). Analyses of N and P concentrations used international standards run blind alongside the samples, and are expressed as N and P content (mmol m^{-2}) in this manuscript due to differences in leaf thickness amongst the species (Table 1). Bulk leaf P_i was determined by extracting samples in 0.3 M TCA at 4˚C before cold centrifuging at 9224 × g (10,000 rpm) for 5 min and collecting

the filtrate (Close & Beadle 2004). The P_i concentrations in the samples were determined against standards made with KH_2PO_4 in serial dilution.

RESULTS

The set of species used in this study ranged two-fold in their leaf thickness, and nearly ten-fold in their leaf P content (Table 1). A_{net} varied more than two-fold, between 10 and 26 μmol m^{-2} s^{-1} among the species when measured at C_i between 27-28 Pa. As a stoichiometric index of P versus N limitation, six of the ten species studied had N:P ratios > 20, while *E. fastigata* and *L. styraciflua*, both from moderately-fertile conditions, had N:P of 10-13 (see Supporting Information, Table S1).

Biochemical modelling from A_{net} - C_c response curves at both 21 and 2 kPa pO_2 using the classic FvCB model would suggest a slightly higher A_{net} asymptote at high C_c and low pO_2 (i.e. similar A_{max} at ambient and low pO_2) due to the lower Γ^* as per Eqn 5 above (Fig. 2). Thus, a stimulation of A_{net} by low pO_2 was expected both in the carboxylation-limited region of the CO_2-response curve and, though smaller, also in the RuBP-regeneration-limited region or where A_{net} is saturated with respect to C_a. Consistent with this, there was an average of 23% stimulation in A_{net} at ambient CO_2 under low-photorespiratory conditions using 2 kPa pO_2 in the carboxylation-limited region of the A_{net} - C_c response curve (Fig. 3 and data not shown). However, in contrast to theoretical expectations, none of the ten species measured showed the expected small A_{net} stimulation in the RuBP-regeneration-limited region in 2 kPa pO_2 compared with A_{net} in normal pO_2. Rather, species either showed similar A_{max} values as asymptotes to the A_{net} - C_c response in 2 kPa pO_2 compared with 21 kPa pO_2 (Fig. 3A,B), or a dramatic reverse response for the A_{max} in 2 versus 21 kPa pO_2 (Fig. 3C,D), with about a 20% reduction in A_{max} at 2 kPa pO_2 compared with normal pO_2. The cross-over between curves at normal and low pO_2 occurred at C_i values as low as 28 Pa, up to 40 Pa depending on species. In low pO_2 there was also a sharp transition between Rubisco-limited photosynthesis at low C_c and RuBP-regeneration and T_p limited photosynthesis compared to normal pO_2 (Fig. 3). For our study species, the difference in A_{max} between normal and low pO_2 was between 2 and 14 μmol m^{-2} s^{-1} (average of 5.8 μmol m^{-2} s^{-1}), with low pO_2 values consistently lower. This was significantly different from zero for all species, even for *B. attenuata* (P=0.017 in a one-tailed t-test) and *P. levis* (P = 0.01), both

of which had rather small mean differences in asymptotic A_{net} between normal and low pO_2 of about 2 μmol m^{-2} s^{-1} (Fig. 3A,B). This result establishes that there was a reverse sensitivity of A_{net} to the reduction in pO_2 at high C_c across the range of species measured in the field. Given that this reverse sensitivity in low pO_2 conditions was significant in all species, we considered it valid to use the model of Harley & Sharkey (1991) to estimate the P limitation component of the biochemical model, rather than the simpler model of Sharkey (1985) that has been recommended to standardise model fitting.

Estimates of V_{cmax} from independent gas-exchange measurements at either pO_2 level were similar (Fig. 4A). However, we could not recover the same A_{max} in different pO_2 levels using the traditional two-parameter FvCB photosynthesis model (Fig. 4B). The A_{max} estimated in low pO_2 was lower than expected based on A_{max} in normal pO_2 (under the 1:1 line in Fig. 4B). The largest A_{max} reductions in low pO_2 were in species with high A_{max} at normal pO_2, such as *E. fastigata* and *L. styraciflua* (average of 8 and 12 μmol m^{-2} s^{-1} lower, respectively). This was further evidence that an additional parameter to the FvCB photosynthesis model was needed to fit photosynthesis to our field measurements. The difference in modelled A_{max} using the traditional FvCB model to the A_{max} predicted by the model revision proposed by Harley & Sharkey (1991) was largest for species with high A_{max} in normal air (21 kPa pO_2; Fig. 4C). Fitting the T_p parameter using Eqn 7 proposed by Harley & Sharkey (1991) to the data, we were able to recover the A_{max} that we had measured in low pO_2 (Fig. 4D). Taken together, all species showed a reduced A_{max} at low pO_2, with the largest reductions occurring in species with the highest A_{max}. These reductions were recovered once the T_p parameter (Eqn 7) was employed in the model fits.

The difference in A_{max} for the model without T_p considered versus the model with T_p considered was positively correlated with leaf P_i content up to a threshold of about 2 mmol P_i m^{-2} ($r^2 = 0.4$, $P < 0.0001$), beyond which there was no apparent relationship (Fig. 5). There was a similar but weaker relationship ($r^2 = 0.2$) for total T_p below a threshold of ~10 mmol P m^{-2} (not shown). T_p was itself only very weakly correlated with leaf P_i content up to a threshold of 2 mmol P_i m^{-2} ($r^2 = 0.10$, $P < 0.01$; data not shown). Six species (*A. oblongifolia*, *B. attenuata*, *B. serrata*, *E. todtiana*, *E. tereticornis* and *P. levis*) all had leaf P_i contents in the linear region, where the magnitude of suppression of CO_2-saturated photosynthesis by low pO_2 varied strongly with P_i. *E. fastigata* and *L. styraciflua* both had high leaf P_i contents and high A_{max} differences,

443 falling in the saturating region of Fig. 5. The amount of total leaf P present as P_i averaged
444 30 ± 2% (mean ± s.e.) among the species in our study. *Liquidambar styraciflua* had the
445 highest free P_i in leaves, at 46 ± 4% of total leaf P concentration. *B. attenuata*, *B. serrata*
446 and *P. levis* had the lowest total leaf P concentrations (around 0.35 mg P g^{-1}; Table S1),
447 but similar P_i fractions as the species average above.
448 For the set of ten species across a range in soils and P supply levels, the
449 individual photosynthetic model components V_{cmax}, J_{max}, and T_p were all correlated with
450 leaf chemical traits, though correlations with total leaf P_{area} were strongest (Table 2, Fig.
451 6). The three species from Davies Park in the Blue Mountains of NSW had the lowest leaf
452 P_{area} closely followed by those from Lesueur National Park in Western Australia. The
453 strongest relationship between the biochemical components of leaf photosynthetic
454 capacity and leaf chemistry was between J_{max} and leaf P_{area} (R^2 = 0.66, Fig. 6c). Bivariate
455 relationships between photosynthetic model components and leaf N_{area} were not
456 significant (P > 0.10, Table 2), nor was A_{max} associated with leaf N_{area} across the set of
457 species. There were no significant relationships between any of these traits and M_a.
458 V_{omax} was not significantly correlated with N_{area}, and was only marginally significantly
459 correlated with P_{area} (P = 0.052; Table 2 and Fig. 6b). V_{omax} fit to data at both
460 measurement pO_2 levels was significantly correlated with V_{cmax} fit to measurements at
461 both pO_2 (P = 0.0052; not shown) with a slope of 0.17 and a significant y-intercept.

462 **DISCUSSION**

463

464 Reductions in A_{max} during exposure to low pO_2 have been documented for over 50 years
465 (Joliffe & Tregunna 1968), but have rarely been measured in the field. Despite
466 suppression of photorespiration by low pO_2 at the current atmospheric C_a (Fig. 2), we
467 have shown that A_{net} at high C_i and low pO_2 is reduced, rather than higher as would be
468 expected from theory based on the biochemical regulation of photosynthesis (Farquhar
469 *et al.* 1980; Laing *et al.* 1974; von Caemmerer & Farquhar 1981). All ten tree and shrub
470 species studied at a range of Australian sites showed this response to varying degrees,
471 at moderate summertime temperatures (Fig. 4). According to the Harley & Sharkey
472 (1991) theoretical model, when leaves operate at near-saturating C_i, photorespiratory
473 glycerate may not completely re-enter the PCR cycle, so that P_i released by phospho-
474 glycolate phosphatase in the chloroplast, that would normally have been used by the

glycerate kinase reaction upon photorespiratory C return to the chloroplast, is instead available in the stroma for RuBP regeneration (Fig. 1, B). Under low-photorespiratory conditions, this additional source of P_i becomes unavailable, resulting in slower RuBP regeneration and lower A_{max} at low pO_2 than at normal pO_2. Modelling using the equation for T_p in Harley & Sharkey (1991) gives A_{max} results that are broadly consistent with our data (Fig. 4). While limitations to photosynthesis by triose-P utilisation are considered to be uncommon and are often ignored in photosynthetic model-fitting, our field measurements under low-photorespiratory conditions show that T_p can be limiting A_{max} in a wide range of woody species.

An alternative hypothesis for T_p limitations to A_{max} suggests that excessive synthesis of triose-P to be exported from the chloroplast increases recycling of P_i entering chloroplasts, with higher stromal P_i leading to the accumulation of 3PGA and decreasing phosphoglucoisomerase activity and suppressing starch synthesis (Sharkey 1985; Stitt *et al.* 2010; Fig. 1, A). While simpler in concept and in formulation (Eqn 6), the T_p limitation emerging from conservative C cycling back to the chloroplast cannot explain what we found here, because it describes pO_2-insensitive photosynthesis, whilst we found a strong reverse sensitivity of A_{max} to low pO_2 which is only predicted by the Harley & Sharkey (1991) model of T_p limitation. Previous treatments using the Sharkey (1985) formulation did not conduct measurements at low pO_2 at a range of C_a levels, and thus have not been able to distinguish between pO_2-insensitive and reverse-sensitive photosynthesis.

On the basis of the Harley & Sharkey (1991) model, our data provide strong evidence that not only is photorespiration a source of amino acids through NH_3 release in glycine metabolism (Wingler *et al.* 2000), but also that glycolate diversion from re-entry into the chloroplast during photorespiration simultaneously frees stromal P_i to permit enhanced photophosphorylation and RuBP regeneration, thus permitting high A_{max}. Measurements of this phenomenon on a much broader set of C_3 plant species is needed to understand the generality of this phenomenon, but the set of species we studied represents a range of phylogenies and includes species with different affinities for growing on low-P sites. All these species showed significant decreases in A_{max} measured during transient non-photorespiratory conditions. The decreases in A_{max} in low pO_2 for *L. styraciflua*, *E. fastigata* and *E. dunnii* were all greater than 5 μmol m^{-2} s^{-1} and as high as 12 μmol m^{-2} s^{-1} (in *E. fastigata*), and thus were much larger than those of

508 the order of 2 μmol m^{-2} s^{-1} shown for soybean in Harley & Sharkey (1991). Therefore,
509 we suggest that this phenomenon may be common amongst a number of plant genera,
510 and potentially across a significant geographic expanse. There is a need for broader
511 consideration of this mechanism among species, as currently T_p limitations to A_{max} are
512 ascribed to the parameter J_{max} in a large number of studies (for example, Kattge *et al.*
513 2009; Manter & Kerrigan 2004; Walker *et al.* 2014). We also suggest that the
514 mechanism proposed by Harley & Sharkey (1991) is more properly called phosphate
515 limitation rather than triose-P limitation, since triose-P is not necessarily integral to the
516 proposed mechanism (see Fig. 1, B). Nevertheless, we have retained the terminology of
517 Harley & Sharkey (1991) in fitting Eqn 7, but suggest that T_p can be more broadly
518 considered as phosphate limitation to A_{net}.

519 Internal recycling of P_i in cells is important for the balanced production of ATP
520 and regeneration of RuBP as essential requirements for high CO_2-assimilation rates.
521 While a source for P_i for photophosphorylation to regenerate RuBP as depicted in Fig. 1
522 (see B in Fig. 1) could be a valuable mechanism for sustaining A_{net} at high C_i in plants in
523 conditions with limiting soil P, our measurements do not suggest this occurs at the
524 extremely low P levels characterising both the Lesueur National Park and Davies Park
525 sites. Among the ten woody species we measured including some on infertile sites with
526 low soil P-availabilities, plants with low leaf P concentrations (total leaf P < 400 μg g^{-1},
527 for instance) also had slow rates of photorespiration and an apparent high fractional
528 return of photorespiratory glycerate to the chloroplast, resulting in a relatively small
529 inhibition of A_{max} in low pO_2 and high C_i (Fig. 3a,b). However, our findings are consistent
530 with the previously-overlooked mechanism of glycerate sequestration during
531 photorespiration may in fact be common in a number of woody species. This
532 mechanism operates at high C_i (but to C_i as low as 28 Pa depending on species; Fig. 3)
533 which means that it is relevant for a substantial fraction of canopy leaves maintained in
534 shade where RuBP regeneration and triose-P supplies may limit A_{net}. It may also be
535 relevant in elevated atmospheric CO_2 concentrations (Campbell & Sage 2006) with a
536 role in increasing the degree of cellular P_i-deficiency with decreased photorespiration,
537 expected as C_a increases in the future. The mechanism hypothesised by Harley &
538 Sharkey (1991) and supported by our data is not yet considered in physiologically-
539 based models used to project plant CO_2 assimilation behaviour into the future (Wang *et*
540 *al.* 2010). Our identification of this mechanism in the field opens an important new area

of research relevant to expected future conditions including elevated [CO_2], and further field measurements of this sort are crucial to help resolve the range of ecological contexts where P_i regulation over A_{max} may be most important.

The hypothesised mechanism for net P_i release in the chloroplast described by Eqn 7 and shown in Fig. 1 requires glycolate exported from the chloroplast to be sequestered, metabolised or exported from the cell, rather than being converted into glycerate for re-entry into the chloroplast. What are the possible mechanisms for this C "diversion" rather than conservation by chloroplast re-entry? Harley & Sharkey (1991) cited ^{14}C labelling evidence to suggest photorespiratory C export by the vascular system to other parts of the plant (Wingler *et al.* 2000), and at least 12% of the amino acid composition of phloem in *Eucalyptus* comprises serine and glycine (Merchant *et al.* 2010), demonstrating that this export is plausible. There are other plausible fates for this C that may also be important (Reumann & Weber 2006). Glycolate and glyoxylate products of photorespiration (Fig. 1; Wingler *et al.* 2000) can be oxidised by glycolate oxidase in the peroxisome to form oxalic acid, which is stored in vacuoles or metabolised to calcium oxalate crystals, common in a wide range of plants (Franceschi & Nakata 2005) and documented for both *Eucalyptus* and *Acacia* (Brown *et al.* 2013). Alternatively, oxalate might be metabolised again (Havrir 1984) and allow glycerate re-entry into the chloroplast when the requirement for P_i is less. Glycine participates in the early steps of porphyrin synthesis in the mitochondria as part of chlorophyll assembly (Beale 1978) as well as in the synthesis of glutathione, which is involved in stress protection (Wingler et al. 2000). Whilst the ultimate fate of photorespiratory glycolate may vary amongst different plant species, evidence of multiple mechanisms driving a lack of C return to the chloroplast after photorespiratory metabolism provides support for the sequestration of glycolate or its products after photorespiration, a key part of the hypothesised mechanism of Harley & Sharkey (1991).

Some implications of the incomplete photorespiratory glycerate re-entry and subsequent extra available P_i (see B in Fig. 1) are that species with low photorespiration such as Proteaceae (*B. attenuata*, *B. serrata*, *P. levis*; see Supporting Information, Table S1) would have a low flux rate of chloroplastic P_i made available by this mechanism compared with species with higher photorespiration. Some Proteaceae species also allocate more P to their mesophyll cells rather than their epidermal cells (Lambers *et al.* 2015) , compared with other dicots that have relatively high P levels in epidermal cells

574 (Conn & Gilliham 2010). Indeed, five species in our study (*B. attenuata*, *B. serrata*, *E.*
575 *todtiana*, *E. tereticornis* and *P. levis*) all have a leaf P_i content where the magnitude of
576 suppression of A_{max} by low pO_2 varies strongly with P_i (P_i < 2 mmol m^{-2}, Fig. 5). This
577 suggests that at low leaf P contents, these species must rely on existing stromal P_i pools,
578 rather than those saved by the lack of glycerate re-entry during photorespiration at high
579 C_i. Lambers *et al.* (2012) showed that photosynthetic cells of mature *Banksia* leaves
580 extensively replace phospholipids by lipids that do not contain P, i.e. galactolipids and
581 sulfolipids, which reduces their demand for P_i for lipid synthesis and hence increases P_i
582 available for participation in photosynthetic carbon metabolism. Moreover, these
583 species also operate at very low levels of ribosomal RNA (Sulpice *et al.* 2014), which is a
584 major fraction of leaf P (Veneklaas *et al.* 2012). Mechanisms for internal P conservation
585 such as these may obviate the need for P contributed from the lack of photorespiratory
586 glycerate re-entry mechanism in P-impoverished ecosystems.
587 Amongst the species we measured, *L. styraciflua*, *E. saligna* and *E. fastigata*
588 showed the fastest RuBP regeneration rates (i.e. high J_{max}), the highest leaf P_i contents,
589 and also showed the largest decreases in A_{max} at low pO_2. Why do these fast-metabolism
590 plants show an apparently large T_p limitation of A_{max}, when they also have high P_i? The
591 bulk leaf P_i measurements are indicative but inconclusive as only the chloroplastic P_i
592 fraction is relevant to the hypothesised mechanism. The reverse sensitivity to pO_2 at
593 high C_c can occur in species with high photosynthetic activity where the requirement for
594 P_i for ATP synthesis is balanced against the need to maintain low P_i for starch and
595 sucrose synthesis (Sharkey & Vassey 1989). With rapid triose-P production in
596 photosynthesis exceeding the capacity to use triose-P in such species, low pO_2 would
597 decrease photorespiration and reduce P_i from dephosphorylation of phosphoglycolate
598 as well as greatly reduce carbon leaving the Calvin-Benson cycle by serine and/or
599 glycine export. It is not clear yet if these two mechanisms are mutually exclusive, but
600 they are consistent with the data in Figure 5.
601 There is an additional possibility that the T_p limitation of species with high A_{max}
602 may occur due to the high P requirements in such species for ribosomal RNA (rRNA),
603 which is needed to support rapid rates of protein synthesis and growth (Matzek &
604 Vitousek 2009; Niklas *et al.* 2005). The P contained in RNA, particularly rRNA, is a
605 significant fraction of the total non-vacuolar P in leaves (Raven 2012). Hence, if high P
606 costs of rRNA for protein turnover are necessary to support rapid photosynthesis in

mature leaves as suggested by Veneklaas *et al.* (2012) and others (Matzek & Vitousek 2009), then this protein synthesis may be achieved from two concurrent photorespiratory products. Amino acids are generated from photorespiratory ammonia (NH_3) release in glycine decarboxylation (Wingler *et al.* 2000), and the lack of photorespiratory glycerate re-entering the chloroplast frees chloroplastic ATP for enhancing RuBP regeneration and increasing A_{max}, while also freeing P_i for P-rich ribosomes to generate proteins in the stroma (Fig. 1). How much glycine or serine is directed away from the photorespiratory pathway and chloroplast re-entry and rather used for protein biosynthesis is unclear. However, the release of N from photorespiration may be as large as from nitrate reduction (Wingler *et al.* 2000), and hence the release of ATP for RuBP regeneration may also be large (Fig. 3B,D). There is supporting evidence as one of the slow-growing species in our study, *Banksia attenuata*, with low photorespiration (Fig. 3C) was recently demonstrated to have low rRNA concentrations in mature leaves at the Lesueur site (Sulpice *et al.* 2014). We believe that the hypothesis of both N and P release in photorespiration establishes new significance for what has previously been considered to be a "wasteful" process (Busch 2013; Ogren 1984; Wingler *et al.* 2000), but it also requires further investigation. There has been considerable interest in the role of P in limiting photosynthesis and whether P can directly influence leaf photosynthetic capacity (Reich *et al.* 2009). The relationships between biochemical parameters underlying photosynthetic capacity and leaf P content in Fig. 6 across a range in P supply argue for a stronger and more direct role for P in regulating A_{max} in this set of species than for N. Our data have provided evidence of a direct role of P in leaf photosynthetic capacity that is likely not currently realised much since current C_i is often lower than $\sim$ 28 Pa, but could become important with rising C_a. Though the nature and biochemistry of T_p limitations to A_{max} are not fully elucidated, when leaf P concentrations are moderate it appears that the extra photorespiratory source of P_i derived from a net C export from the chloroplast can help sustain rapid rates of A_{max}.

CONCLUSIONS

While triose-P utilisation (T_p) limitations to photosynthesis are considered to be uncommon and are often ignored in photosynthetic model-fitting, we have shown that T_p can be limiting in a wide range of species from across soil P gradients in the field,

639 with short-term high C_i. Hence, what are actually T_p limitations judged from
640 measurements at low pO_2, are currently attributed to J_{max} limitations in the two-phase
641 FvCB model that is frequently fit to measurements at normal pO_2. The results suggest
642 that pO_2 manipulation in measurements of A_{net} can lead to insights into P_i limitations to
643 A_{net} both in the present and in a future with elevated atmospheric CO_2 leading to
644 reduced photorespiration. Intracellular P_i release from photorespiration is inhibited at
645 low pO_2, reducing A_{max} in all species, but to varying extent depending on their available
646 P_i pools. Species with largest photosynthetic capacity and highest P_i contents apparently
647 rely most on ATP made available from photorespiration. Hence, this mechanism is most
648 important in fast-growing species at moderate P levels and with high photosynthetic
649 capacity, rather than species growing in P-impoverished soils. The mechanism we have
650 identified should be further explored, but is expected to contribute to the economy of P
651 for plants in tropical or subtropical rainforest vegetation as well as in Mediterranean
652 vegetation on soils with moderate to low P availability, but not in those species that
653 deploy alternative mechanisms to function at very low leaf [P]. Phosphate limitations to
654 photosynthetic capacity are likely more common in the field than previously thought,
655 and likely contribute to improving the predictability of CO_2-assimilation rates in such
656 instances. It is recommended that those interested in modelling how biochemistry
657 regulates A_{net} should consider the role of photorespiration and employ three limitations
658 in the biochemical model of photosynthesis with the possibility of glycerate not re-
659 entering the Calvin-Benson cycle.

660 ## ACKNOWLEDGEMENTS

661 This research was supported by the Australian Research Council (ARC Discovery grant
662 DP110105102 to DSE and DP110101120 to HL). Data from this study is stored at
663 Research Data Australia (doi: tobedetermined). We are grateful to O.K. Atkin (ANU), K.
664 Bloomfield (Leeds University), and P. Milham (NSW government) for advice concerning
665 the chemical analysis of P_i and total P in leaves. S. Wohl expertly operated the cranes for
666 canopy access at EucFACE. We thank the Blue Mountains City Council (BMCC) and
667 particularly Michael Hensen, for permission to sample at Davies Park in the Blue
668 Mountains, NSW, the staff at the Illawarra Fly for providing access to the canopy
669 walkway in Robertson, NSW, and the Western Australia Department of Parks and
670 Wildlife for sampling access to Lesueur National Park, WA. Further, we thank Prof. Tom

671 Sharkey and two anonymous referees for their very useful comments on an earlier
672 draft. A portion of this work was conducted at the EucFACE facility, an initiative of the
673 Australian Government's economic stimulus package and part of Australia's national
674 collaborative research infrastructure (NCRIS).
675

676 ## REFERENCES

677 Aerts R. & Chapin F.S. (2000) The mineral nutrition of wild plants revisited: a re-
678 evaluation of processes and patterns. *Advances in Ecological Research*, **30**, 1-67.
679 Archontoulis S.V., Yin X., Vos J., Danalotos N.G. & Struick P.G. (2012) Leaf photosynthesis
680 and respiration of three bioenergy crops in relation to temperature and leaf
681 nitrogen: how conserved are biochemical model parameters among crop
682 species? *Journal of Experimental Botany*, **63**, 895–911.
683 Beadle N.C.W. (1966) Soil phosphate and its role in molding segments of the Australian
684 flora and vegetation, with special reference to xeromorphy and sclerophylly.
685 *Ecology*, **47**, 992-1007.
686 Beale S.I. (1978) Delta-aminolevulinic acid in plants - its biosynthesis, regulation, and
687 role in plastid development. *Annual Review of Plant Physiology and Plant*
688 *Molecular Biology*, **29**, 95-120.
689 Bernacchi C.J., Bagley J.E., Serbin S.P., Ruiz-Vera U.M., Rosenthal D.M. & Vanloocke A.
690 (2013) Modelling C3 photosynthesis from the chloroplast to the ecosystem. *Plant*
691 *Cell and Environment*, **36**, 1641–1657.
692 Bernacchi C.J., Singsaas E.L., Pimentel C., Portis A.R. & Long S.P. (2001) Improved
693 temperature response functions for models of Rubisco-limited photosynthesis.
694 *Plant Cell and Environment*, **24**, 253-259.
695 Bonan G.B., Lawrence P.J., Oleson K.W., Levis S., Jung M., Reichstein M., Lawrence D.M. &
696 Swenson S.C. (2011) Improving canopy processes in the Community Land Model

version 4 (CLM4) using global flux fields empirically inferred from FLUXNET data. *Journal of Geophysical Research-Biogeosciences*, **116**.

Bown H.E., Watt M.S., Clinton P.W., Mason E.G. & Richardson B. (2009) Partititioning concurrent influences of nitrogen and phosphorus supply on photosynthetic model parameters of *Pinus radiata*. *Tree Physiology*, **27**, 335-344.

Brooks A. (1986) Effects of phosphorus nutrition on Ribulose-1,5-bisphosphate carboxylase activation, photosynthetic quantum yield and amounts of some Calvin-cycle metabolites in spinach leaves. *Australian Journal of Plant Physiology*, **13**, 221-237.

Brown S.L., Warwick N.W.M. & Prychid C.J. (2013) Does aridity influence the morphology, distribution and accumulation of calcium oxalate crystals in Acacia (Leguminosae: Mimosoideae)? *Plant Physiology and Biochemistry*, **73**, 219-228.

Bunce J.A. (2002) Sensitivity of infrared water vapor analyzers to oxygen concentration and errors in stomatal conductance. *Photosynthesis Research*, **71**, 273–276.

Burch D.E., Singleton E.B. & Williams D. (1962) Absorption line broadening in the infrared. *Applied Optics*, **1**, 359-363.

Busch F.A. (2013) Current methods for estimating the rate of photorespiration in leaves. *Plant Biology*, **15**, 648-655.

Campbell C.D. & Sage R.F. (2006) Interactions between the effects of atmospheric CO_2 content and P nutrition on photosynthesis in white lupin (*Lupinus albus* L.). *Plant Cell and Environment*, **29**, 844-853.

Cernusak L.A., Hutley L.B., Beringer J., Holtum J.A. & Turner B.L. (2011) Photosynthetic physiology of eucalypts along a sub-continental rainfall gradient in northern Australia. *Agricultural and Forest Meteorology*, **151**, 1462-1470.

721 Close D.G. & Beadle C.L. (2004) Total, and chemical fractions, of nitrogen and
722 phosphorus in *Eucalyptus* seedling leaves: Effects of species, nursery fertiliser
723 management and transplanting. *Plant and Soil*, **259**, 85-95.
724 Conn S. & Gilliham M. (2010) Comparative physiology of elemental distributions in
725 plants. *Annals of Botany*, **105**, 1081-1102.
726 Crous K.Y., Quentin A.G., Lin Y.-S., Medlyn B.E., Williams D.G., Barton C.V.M. & Ellsworth
727 D.S. (2013) Photosynthesis of temperate *Eucalyptus globulus* trees outside their
728 native range has limited adjustment to elevated CO_2 and climate warming. *Global*
729 *Change Biology*, **19**, 3790–3807.
730 Denton M.D., Veneklaas E.J., Freimoser F.M. & Lambers H. (2007) *Banksia* species
731 (Proteaceae) from severely phosphorus-impoverished soils exhibit extreme
732 efficiency in the use and re-mobilization of phosphorus. *Plant Cell and*
733 *Environment*, **30**, 1557-1565.
734 Domingues T.F., Meir P., Feldpausch T., Saiz G., Venendaal E.M., Schrodt F., Bird M.,
735 Djagblety G., Hien F., Camapore H., Diallo A., Grace J. & Lloyd J. (2010) Co-
736 limitation of photosynthetic capacity by nitrogen and phosphorus in West Africa
737 woodlands. *Plant Cell and Environment*, **33**, 959-980.
738 Ellsworth D.S., Reich P.B., Naumburg E.S., Koch G.W., Kubiske M.E. & Smith S.D. (2004)
739 Photosynthesis, carboxylation and leaf nitrogen responses of 16 species to
740 elevated pCO_2 across four free-air CO_2 enrichment experiments in forest,
741 grassland and desert. *Global Change Biology*, **10**, 2121-2138.
742 Ellsworth D.S., Thomas R.B., Crous K.Y., Palmroth S., Ward E., Maier C., DeLucia E.H. &
743 Oren R. (2012) Elevated CO_2 affects photosynthetic responses in canopy pine and
744 subcanopy deciduous trees over 10 years: a synthesis from Duke FACE. *Global*
745 *Change Biology*, **18**, 223–242.

746 Evans J.R. (1989) Photosynthesis and nitrogen relationships in leaves of C3 plants.
747 *Oecologia*, **78**, 9-19.
748 Farquhar G.D., Caemmerer S.V. & Berry J.A. (1980) A biochemical model of
749 photosynthetic CO_2 assimilation in leaves of C3 species. *Planta*, **149**, 78-90.
750 Farquhar G.D., von Caemmerer S. & Berry J.A. (2001) Models of photosynthesis. *Plant*
751 *Physiology*, **125**, 42-45.
752 Flexas J., Barbour M.M., Brendel O., Cabrera H.M., Carriqui M., Diaz-Espejo A., Douthe C.,
753 Dreyer E., Ferrio J.P., Gago J., Galle A., Galmés J., Kodama N., Medrano H.,
754 Niinemets Ü., Peguero-Pina J.J., Pou A., Ribas-Carbo M., Tomas M., Tosens T. &
755 Warren C.R. (2012) Mesophyll diffusion conductance to CO_2: An unappreciated
756 central player in photosynthesis. *Plant Science*, **193**, 70-84.
757 Franceschi V.R. & Nakata P.A. (2005) Calcium oxalate in plants: formation and function.
758 *Annual Review of Plant Biology*, **56**, 41-71.
759 Galmés J., Flexas J., Keys A.J., Cifre J., Mitchell R.A.C., Madgwick P.J., Haslam R.P., Medrano
760 H. & Parry M.A.J. (2005) Rubisco specificity factor tends to be larger in plant
761 species from drier habitats and in species with persistent leaves. *Plant Cell and*
762 *Environment*, **28**, 571-579.
763 Griffin E.A. & Burbidge A.A. (1990) Description of the region. In: *Nature Conservation,*
764 *Landscape and Recreational Values of the Lesueur Area.* (eds A.A. Burbidge, S.D.
765 Hopper, & D. Van Leeuwen), pp. 15-24. Environmental Protection Authority,
766 Perth, WA Australia.
767 Groenendijk M., Dolman A.J., van der Molen M.K., Leuning R., Arneth A., Delpierre N.,
768 Gash J.H.C., Lindroth A., Richardson A.D., Verbeeck H. & Wohlfahrt G. (2011)
769 Assessing parameter variability in a photosynthesis model within and between

plant functional types using global Fluxnet eddy covariance data. *Agricultural and Forest Meteorology*, **151**, 22-38.

Gu L. & Sun Y. (2014) Artefactual responses of mesophyll conductance to CO_2 and irradiance estimated with the variable J and online isotope discrimination methods. *Plant Cell and Environment*, **37**, 1231-1249.

Hammond J.P. & White P.J. (2011) Sugar signaling in root responses to low phosphorus availability. *Plant Physiology*, **156**, 1033-1040.

Harley P.C. & Sharkey T.D. (1991) An improved model of C_3 photosynthesis at high CO_2: reversed O_2 sensitivity explained by lack of glycerate reentry into the chloroplast. *Photosynthesis Research*, **27**, 169-178.

Havrir E.A. (1984) Oxalate metabolism by tobacco leaf discs. *Plant Physiology*, **75**, 505-507.

Holford I.C.R. (1997) Soil phosphorus: its measurement, and its uptake by plants. *Australian Journal of Soil Research*, **35**, 227-239.

Jacob J. & Lawlor D.W. (1993) In vivo photosynthetic electron transport does not limit photosynthetic capacity in phosphate deficient sunflower and maize leaves. *Plant Cell and Environment*, **16**, 785–795.

Joliffe P.A. & Tregunna E.B. (1968) Effect of temperature, CO_2 concentration, and light intensity on oxygen inhibition of photosynthesis in wheat leaves. *Plant Physiology*, **43**, 902-906.

Kattge J., Knorr W., Raddatz T. & Wirth C. (2009) Quantifying photosynthetic capacity and its relationship to leaf nitrogen content for global-scale terrestrial biosphere models. *Global Change Biology*, **15**, 976–991.

793 Laing W.A., Ogren W.L. & Hageman R.H. (1974) Regulation of soybean net
794 photosynthetic CO_2 fixation by interaction of CO_2, O_2, and ribulose 1,5-
795 diphosphate carboxylase. *Plant Physiology*, **54**, 678-685.
796 Lambers H., Brundrett M.C., Raven J.A. & Hopper S.D. (2010) Plant mineral nutrition in
797 ancient landscapes: high plant species diversity on infertile soils is linked to
798 functional diversity for nutritional strategies. *Plant and Soil*, **334**, 11–31.
799 Lambers H., Cawthray G.R., Giavalisco P., Kuo J., Laliberté E., Pearse S.J., Scheible W.R.,
800 Stitt M., Teste F. & Turner B.L. (2012) Proteaceae from severely phosphorus-
801 impoverished soils extensively replace phospholipids with galactolipids and
802 sulfolipids during leaf development to achieve a high photosynthetic
803 phosphorus-use-efficiency. *New Phytologist*, **196**, 1098-1108.
804 Lambers H., Clode P., Hawkins H.-J., Laliberté E., R.S. O., Reddell P., Shane M.W., Stitt M. &
805 Weston P. (2015) Metabolic adaptations of the non-mycotrophic Proteaceae to
806 soils with low phosphorus availability. In: *Phosphorus Metabolism in Plants in the*
807 *Post-genomic Era: From Gene to Ecosystem.* (eds W.C. Plaxton & H. Lambers), pp.
808 1-44. Wiley-Blackwell, London.
809 Li-Cor (2008) Using the Li-6400/Li-6400XT Portable Photosynthesis System. Li-Cor,
810 Lincoln, NE USA.
811 Long S.P. & Bernacchi C. (2003) Gas exchange measurements, what can they tell us
812 about the underlying limitations to photosynthesis? Procedures and sources of
813 error. *Journal of Experimental Botany*, **54**, 2393-2401.
814 Loustau D., Brahim M.B., Gaudillere J.-P. & Dreyer E. (1999) Photosynthetic responses to
815 phosphorus nutrition in two-year-old maritime pine seedlings. *Tree Physiology*,
816 **19**, 707-715.

817 Manter D.K. & Kerrigan J. (2004) A/C-i curve analysis across a range of woody plant
818 species: influence of regression analysis parameters and mesophyll conductance.
819 *Journal of Experimental Botany*, **55**, 2581-2588.
820 Matzek V. & Vitousek P.M. (2009) N : P stoichiometry and protein : RNA ratios in
821 vascular plants: an evaluation of the growth-rate hypothesis. *Ecology Letters*, **12**,
822 765-771.
823 Merchant A., Peuke A.D., Keitel C., Macfarlane C., Warren C.R. & Adams M.A. (2010)
824 Phloem sap and leaf $\delta^{13}C$, carbohydrates, and amino acid concentrations in
825 *Eucalyptus globulus* change systematically according to flooding and water deficit
826 treatment. *Journal of Experimental Botany*, **61**, 1785–1793.
827 Niklas K.J., Owens T., Reich P.B. & Cobb E.D. (2005) Nitrogen / phosphorus leaf
828 stoichiometry and the scaling of plant growth. . *Ecology Letters*, **8**, 636–642.
829 Ogren W.L. (1984) Photorespiration: pathways, regulation, and modification. *Annual*
830 *Review of Plant Physiology*, **35**, 415-442.
831 Paul M.J. & Foyer C.H. (2001) Sink regulation of photosynthesis. *Journal of Experimental*
832 *Botany*, **52**, 1383-1400.
833 Piao S.L., Sitch S., Ciais P., Friedlingstein P., Peylin P., Wang X.H., Ahlstrom A., Anav A.,
834 Canadell J.G., Cong N., Huntingford C., Jung M., Levis S., Levy P.E., Li J.S., Lin X.,
835 Lomas M.R., Lu M., Luo Y.Q., Ma Y.C., Myneni R.B., Poulter B., Sun Z.Z., Wang T.,
836 Viovy N., Zaehle S. & Zeng N. (2013) Evaluation of terrestrial carbon cycle models
837 for their response to climate variability and to CO_2 trends. *Global Change Biology*,
838 **19**, 2117-2132.
839 Pieters A.J., Paul M.J. & Lawlor D.W. (2001) Low sink demand limits photosynthesis
840 under P_i deficiency. *Journal of Experimental Botany*, **52**, 1083-1091.

841 Pons T., Flexas J., von Caemmerer S., Evans J.R., Genty B., Ribas-Carbo M. & Brugnoli E.
842 (2009) Estimating mesophyll conductance to CO_2: methodology, potential errors,
843 and recommendations. *Journal of Experimental Botany*, **60**, 2217–2234.
844 Raven J.A. (2012) Protein turnover and plant RNA and phosphorus requirements in
845 relation to nitrogen fixation. *Plant Science*, **188**, 25-35.
846 Reich P.B., Oleksyn J. & Wright I.J. (2009) Leaf phosphorus influences the
847 photosynthesis-nitrogen relation: a cross-biome analysis of 314 species.
848 *Oecologia*, **160**, 207-212.
849 Reumann S. & Weber A.P.M. (2006) Plant peroxisomes respire in the light: some gaps of
850 the photorespiratory C_2 cycle have become filled - others remain. *Biochim*
851 *Biophys Acta*, **1763**, 1496–1510.
852 Rogers A. (2014) The use and mis-use of $V_{c,max}$ in earth system models. *Photosynthesis*
853 *Research*, **119**, 15-29.
854 Sage R.F. & Sharkey T.D. (1987) The effect of temperature on the occurrence of O_2 and
855 CO_2-insensitive photosynthesis in field grown plants. *Plant Physiology*, **84**, 658-
856 664.
857 Sharkey T.D. (1985) Photosynthesis in intact leaves of C3 plants - physics, physiology
858 and rate limitations. *Botanical Review*, **51**, 53-105.
859 Sharkey T.D. (1988) Estimating the rate of photorespiration in leaves. *Physiologia*
860 *Plantarum*, **73**, 147-152.
861 Sharkey T.D., Bernacchi C.J., Farquhar G.D. & Singsaas E.L. (2007) Fitting photosynthetic
862 carbon dioxide response curves for C3 leaves. *Plant Cell and Environment*, **30**,
863 1035-1040.
864 Sharkey T.D. & Vassey T.L. (1989) Low oxygen inhibition of photosynthesis is caused by
865 inhibition of starch synthesis. *Plant Physiology*, **90**, 385-387.

Stitt M., Lunn J. & Usadel B. (2010) *Arabidopsis* and primary photosynthetic metabolism – more than the icing on the cake. *Plant Journal*, **61**, 1067-1091.

Sulpice R., Ishihara H., Schlereth A., Cawthray G.R., Encke B., Giavalisco P., Ivakov A., Arrivault S., Jost R., Krohn N., Kuo J., Laliberte E., Pearse S.J., Raven J.A., Scheible W.R., Teste F., Veneklaas E.J., Stitt M. & Lambers H. (2014) Low levels of ribosomal RNA partly account for the very high photosynthetic phosphorus-use efficiency of Proteaceae species. *Plant Cell and Environment*, **37**, 1276-1298.

Tazoe Y., von Caemmerer S., Estavillo G.M. & Evans J.R. (2011) Using tunable diode laser spectroscopy to measure carbon isotope discrimination and mesophyll conductance to CO_2 diffusion dynamically at different CO_2 concentrations. *Plant Cell and Environment*, **34**, 580-591.

R Core Development Team (2014) A language and environment for statistical computing. R Foundation for Statistical Computing, Vienna, Austria. http://www.R-project.org.

Thomas D.S., Montagu K.D. & Conroy J.P. (2006) Leaf inorganic phosphorus as a potential indicator of phosphorus status, photosynthesis and growth of *Eucalyptus grandis* seedlings. *Forest Ecology and Management*, **223**, 267–274.

Veneklaas E.J., Lambers H., Bragg J., Finnegan P.M., Lovelock C.E., Plaxton W.C., Price C.A., Scheible W.R., Shane M.W., White P.J. & Raven J.A. (2012) Opportunities for improving phosphorus-use efficiency in crop plants. *New Phytologist*, **195**, 306-320.

Vitousek P.M., Porder S., Houlton B.Z. & Chadwick O.A. (2010) Terrestrial phosphorus limitation: mechanisms, implications, and nitrogen-phosphorus interactions. *Ecological Applications*, **20**, 5-15.

890 von Caemmerer S. (2000) *Biochemical Models of Leaf Photosynthesis.* CSIRO Publishing,
891 Collingwood, Victoria, Australia.
892 von Caemmerer S. (2013) Steady-state models of photosynthesis. *Plant Cell and*
893 *Environment*, **36**, 1617-1630.
894 von Caemmerer S. & Farquhar G.D. (1981) Some relationships between the
895 biochemistry of photosynthesis and the gas exchange of leaves. *Planta*, **153**, 376-
896 387.
897 Walker A.P., Beckerman A.P., Gu L., Kattge J., Cernusak L.A., Domingues T.F., Scales J.C.,
898 Wohlfahrt G., Wullschleger S.D. & Woodward F.I. (2014) The relationship of leaf
899 photosynthetic traits - Vcmax and Jmax - to leaf nitrogen, leaf phosphorus, and
900 specific leaf area: a meta-analysis and modeling study. *Ecology and Evolution*, **4**,
901 3218-3235.
902 Walker B., Ariza L.S., Kaines S., Badger M.R. & Cousins A.B. (2013) Temperature
903 response of *in vivo* Rubisco kinetics and mesophyll conductance in *Arabidopsis*
904 *thaliana*: comparisons to *Nicotiana tabacum*. *Plant Cell and Environment*, **36**,
905 2108-2119.
906 Wang Y.P., Law R.M. & Pak B. (2010) A global model of carbon, nitrogen and phosphorus
907 cycles for the terrestrial biosphere. *Biogeosciences*, **7**, 2261-2282.
908 Williams M., Rastetter E.B., Fernandes D.N., Goulden M.L., Shaver G.R. & Johnson L.C.
909 (1997) Predicting gross primary productivity in terrestrial ecosystems.
910 *Ecological Applications*, **7**, 882-894.
911 Wingler A., Lea P.J., Quick W.P. & Leegood R.C. (2000) Photorespiration: metabolic
912 pathways and their role in stress protection. *Philosophical Transactions of the*
913 *Royal Society London Series B*, **355**, 1517-1529.

914 Yang X. & Post W.M. (2011) Phosphorus transformations as a function of pedogenesis: a
915 synthesis of soil phosphorus data using Hedley fractionation method.
916 *Biogeosciences*, **8**, 2907-2916.
917 Zaehle S., Medlyn B.E., De Kauwe M.G., Walker A.P., Dietze M.C., Hickler T., Luo Y.Q.,
918 Wang Y.P., El-Masri B., Thornton P., Jain A., Wang S.S., Warlind D., Weng E.S.,
919 Parton W., Iversen C.M., Gallet-Budynek A., McCarthy H., Finzi A., Hanson P.J.,
920 Prentice I.C., Oren R. & Norby R.J. (2014) Evaluation of 11 terrestrial carbon-
921 nitrogen cycle models against observations from two temperate Free-Air CO_2
922 Enrichment studies. *New Phytologist*, **202**, 803-822.
923
924

Table 1. Description of species and sites included in the study along with number of individuals measured (N), the mean height that measurements were taken at, and the mean leaf thickness, leaf dry mass-to-area ratio, and total leaf P concentration per unit leaf area (P_a). Data are means ± s.e. The species name abbreviation is used to denote the different species in the figures.

Species name and abbrev.	Type	Site	Location	N	Height (m)	Leaf thickness (μm)	M_a (g m^{-2})	Leaf P_a (mmol P m^{-2})
Acacia oblongifolia (A. obl)	Native shrub	Davies Park, Springwood, NSW	33º 42' 28" S, 150º 32' 51" E	4	1-2	315	192.5 ± 11.8	2.5 ± 0.5
Banksia attenuata (B. att)	Native shrub	Lesueur National Park, Jurien Bay, WA	30º 11' 02" S, 115º 09' 27" E	3	1	430	271.5 ± 19.5	2.7 ± 0.4
B. serrata (B. ser)	Native shrub	Davies Park, Springwood, NSW	33º 42' 28" S, 150º 32' 51" E	3	1-2	540	207.2 ± 3.7	1.7 ± 0.2
Eucalyptus dunnii (E. dun)	Plantation tree	Hawkesbury Forest Experiment, Richmond NSW	33º 36' 40" S, 150º 44' 27" E	4	10	260	135.6 ± 2.6	6.1 ± 0.5
E. fastigata (E. fas)	Native mature sclerophyll woodland tree	Illawarra escarpment, Robertson, NSW	34° 37' 06" S, 150° 42' 48" E	5	25	300	168.9 ± 10.3	8.2 ± 1.6
E. saligna (E. sal)	Plantation tree	Hawkesbury Forest Experiment, Richmond NSW	33º 36' 40" S, 150º 44' 27" E	3	9	318	147.2 ± 7.3	6.3 ±1.7
E. tereticornis (E. ter)	Native mature sclerophyll woodland tree	Eucalyptus site (EucFACE), Richmond, NSW	33º 36' 57" S, 150º 44' 16" E	3	19	356	208.3 ± 11.7	7.3 ± 0.3
E. todtiana (E. tod)	Native mature woodland tree	Lesueur National Park, Jurien Bay, WA	30º 11' 02" S, 115º 09' 27" E	3	2	530	305.0 ± 4.5	3.8 ± 0.4
Liquidambar styraciflua (L. sty)	Plantation tree	Hawkesbury campus, Richmond, NSW	33º 36' 57" S, 150º 45' 06" E	4	4	237	111.9 ± 2.0	6.6 ±1.5

Persoonia levis (P. lev)	Native shrub	Davies Park, Springwood, NSW	33º 42’ 28” S, 150º 32’ 51” E	4	2	420	167.0 ± 18.8	1.8 ± 0.1

Table 2. Summary of relationships between biochemical parameters of leaf photosynthetic capacity and leaf chemistry for ten species in this study. Leaf N_{area} and P_{area} are expressed in mmol m^{-2}.

Relationship	Equation	Coefficient of determination (R^2)	*P*-value
V_{cmax} by N_{area}	*N.S.*	-	0.874
V_{cmax} by P_{area}	*N.S.*	0.371	0.062
V_{omax} by N_{area}	*N.S.*	-	0.361
V_{omax} by P_{area}	$V_{omax} = 27.66 + 3.54*P_{area}$	0.394	0.052
J_{max} by N_{area}	*N.S.*	-	0.322
J_{max} by P_{area}	$J_{max} = 88.56 + 400.99*P_{area}$	0.656	0.045
T_p by N_{area}	*N.S.*	-	0.201
T_p by P_{area}	$T_p = 6.51 + 14.64*P_{area}$	0.446	0.035

Figure 1. Diagram of the biochemical models hypothesised to account for the O_2 sensitivity of photosynthesis, with emphasis placed on areas indicated by the encircled as A) showing limitations by end-product synthesis (depicted in Eqn 6), and the circle B) showing the hypothesised mechanism from Harley & Sharkey (1991) with emphasis on P_i release by P-glycolate phosphatase and subsequent incomplete photorespiratory glycerate re-entry to the chloroplast (depicted in Eqn 7), resulting in a net increase in stromal P_i for photophosphorylation and RuBP regeneration. The small boxes are membrane-bound transporters.

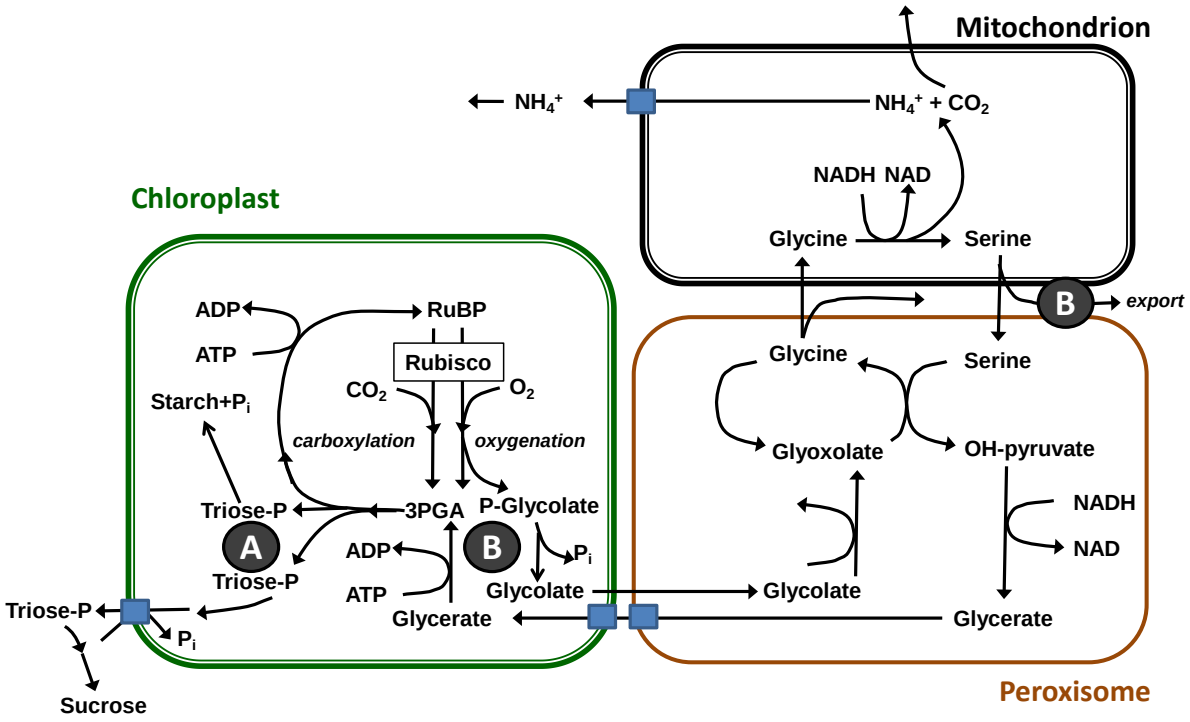

Figure 2. A theoretical depiction of the prediction of A_{net} as a function of the CO_2 partial pressure inside the chloroplast (C_c) (a) for normal O_2 and (b) for low pO_2 predicted by the biochemical model of FvCB, showing the component limitations to A_{net} in colour. Blue dashes show the theoretical A_{net} limited by the maximum capacity for carboxylation, orange dashes shows the theoretical A_{net} limited by electron transport for the regeneration of RuBP in the Calvin-Benson cycle, and green dashes show the theoretical A_{net} limited by triose-phosphate utilisation as per Eqn 6. The dark black line shows the overall relationship between A_{net} and C_c predicted by the minimum of the three limitations. The grey line in (b) represents the black curve in (a) for direct comparison with predictions for low pO_2.

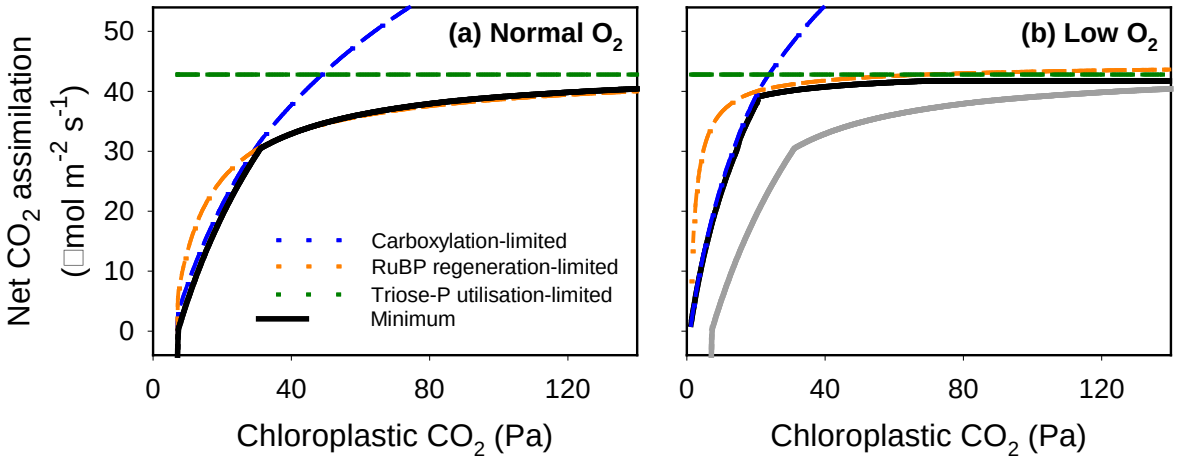

Figure 3. A_{net} as a function of chloroplastic pCO_2 partial pressure (C_c) measured in the field for four woody species examples (*P. levis*, *B. attenuata*, *L. stryraciflua*, and *E. fastigata*, panels a-d, respectively) at both normal (21 kPa, filled light blue symbols) and low pO_2 (2 kPa, open red symbols), with ensemble response curve fits for each species and pO_2 level. Data are for three to four leaves from different trees on which measurements at both pO_2 values had been made (see Table 1). The lines shown represent separate fits of the standard model of Farquhar *et al.* (1980) to all the data at each respective pO_2 for a given species.

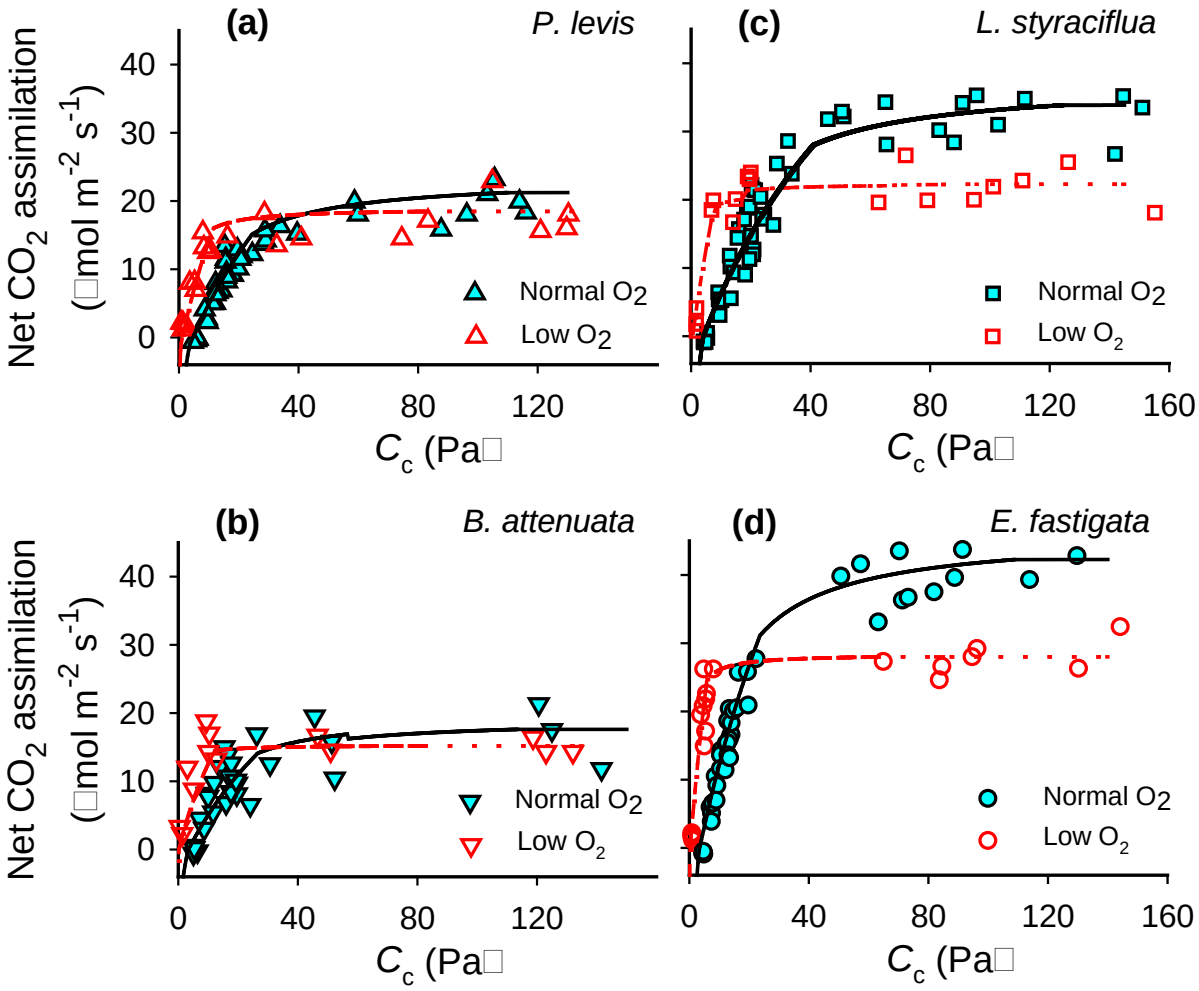

Figure 4. Results of the independent fits of the standard Farquhar *et al*. (1980) model to data at normal versus at low pO_2 for ten species for a) carboxylation capacity (V_{cmax}), b) light- and CO_2-saturated photosynthetic capacity (A_{max}), and c) the A_{max} difference in low pO_2 modelled including T_p limitation versus not including T_p limitation as a function of A_{max} in normal pO_2. Panel (d) shows A_{max} in low pO_2 modelled including T_p limitation as a function of A_{max} measured in normal pO_2. The 1:1 line in panels a,b,d is shown as a dashed line across each panel and the solid line in panel c represents the line delineated by Y = 0.50*x – 6.83, with $r^2 = 0.79$. Species are abbreviated to four letters representing the genus and species names (see Table 1).

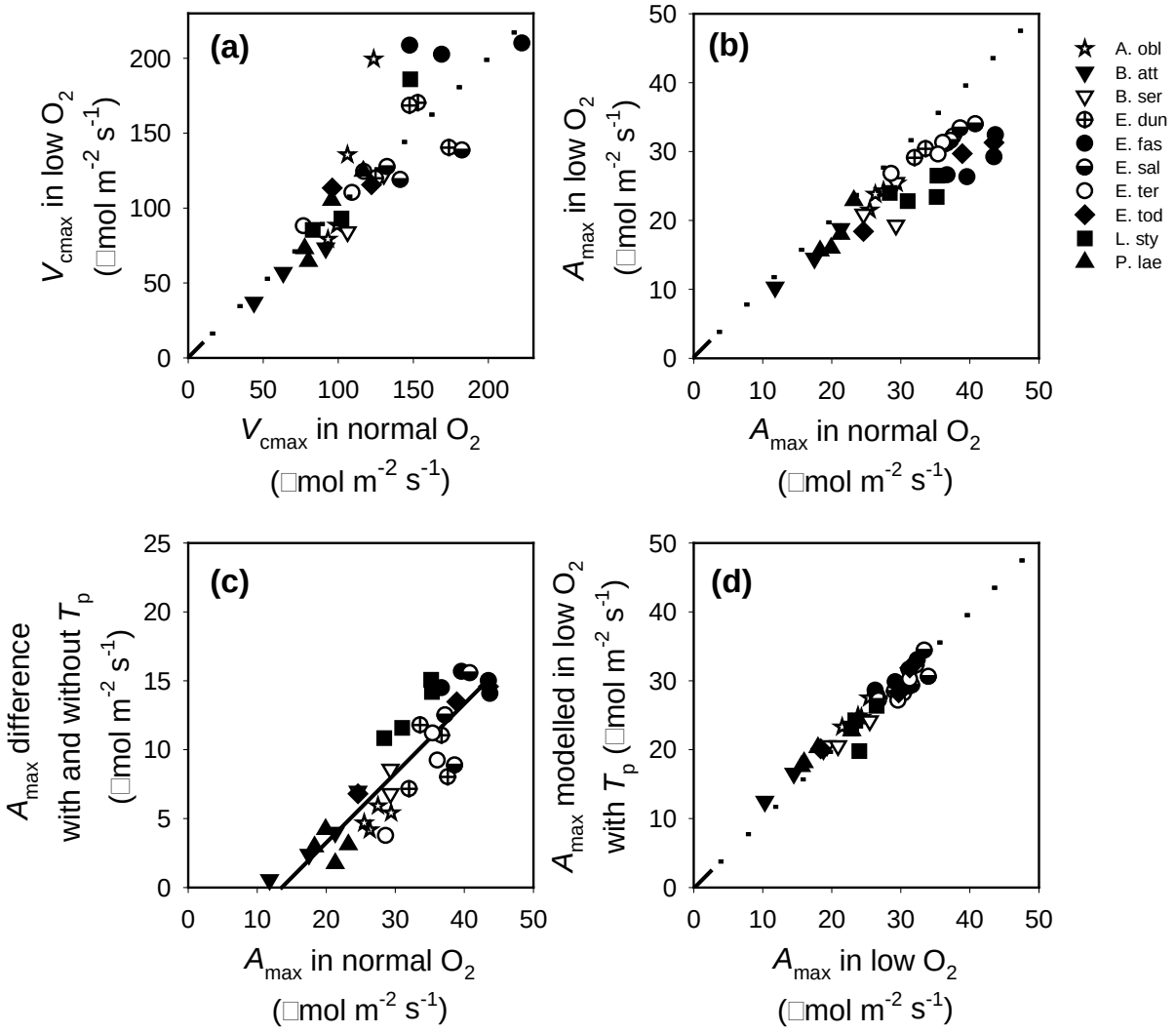

Figure 5. The difference in A_{max} in low pO_2 when modelled including T_p limitation from Eqn 7 versus A_{max} in low pO_2 without T_p limitation considered is shown as a function of bulk leaf inorganic P, P_i. Species abbreviations are given in Table 1.

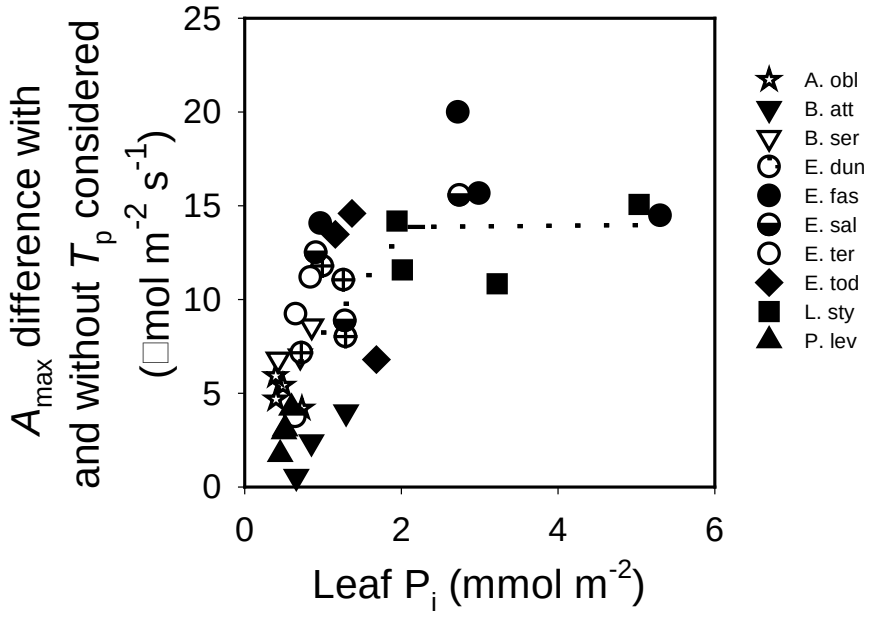

Figure 6. The relationships between four modelled biochemical components of photosynthetic or photorespiratory capacity (V_{cmax}, panel a; V_{omax}, panel b; J_{max}, panel c; T_p, panel d) and leaf P concentration for the ten species studied (abbreviation in Table 1). Each point represents the mean of individuals of a species (see Table 1), fit ensemble. V_{cmax} and V_{omax} species means across different individuals are reported in Supporting Information, Table S1. Dashed lines are shown where the relationships are significant. The data point for *Acacia obtusifolia* is obscured by that of *Banksia serrata* in panel C, as they had very similar J_{max} values. Equations for these relationships are shown in Table 2.

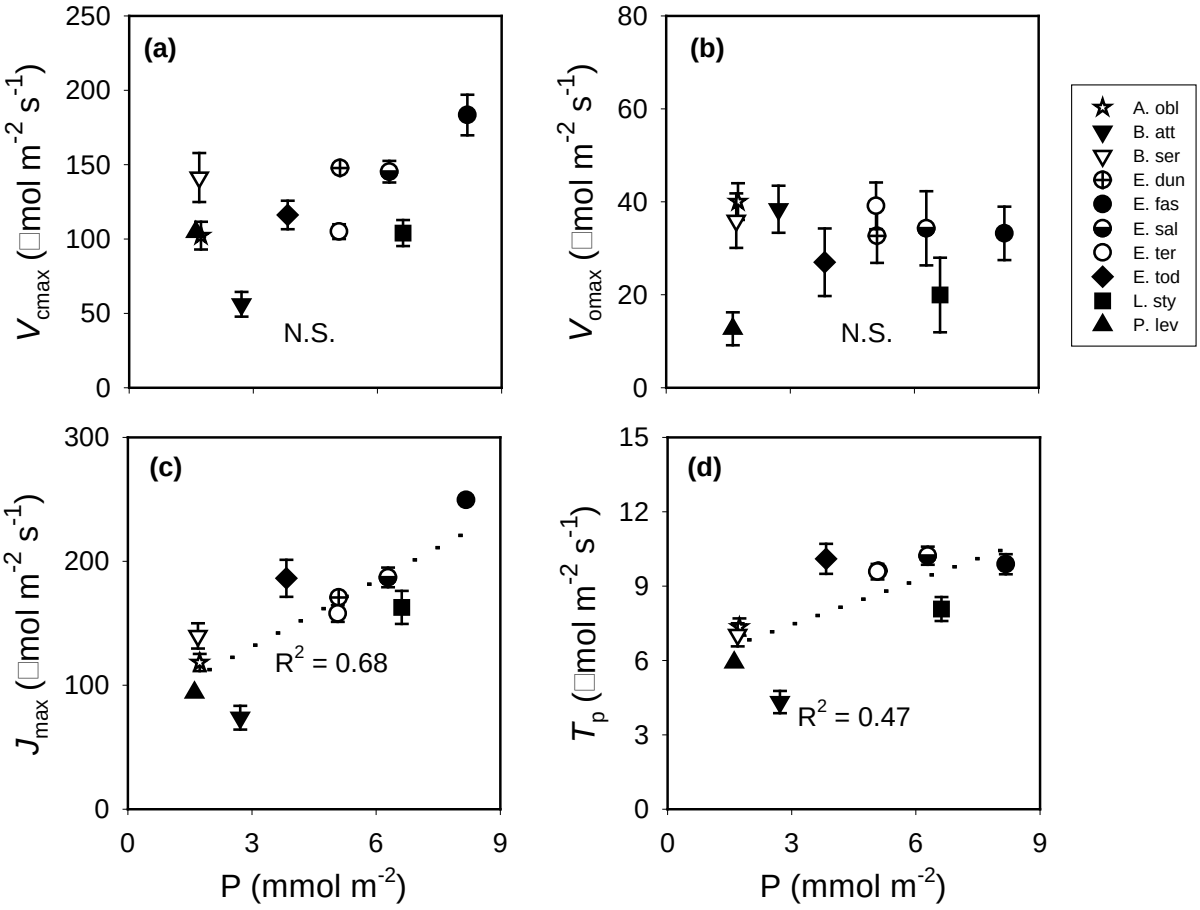

Supporting Information

Table S1. Summary of species means for V_{cmax}, fit using both pO_2 levels up to a C_c threshold of 18 Pa, V_{omax} as a measure of photorespiratory capacity, also fit from data from both pO_2 up to a C_c threshold of 18 Pa, and leaf N and P concentrations and N to P ratios for the ten species in this study. Data are means ± s.e.

Species name	V_{cmax} (µmol CO_2 m^{-2} s^{-1})	V_{omax} (µmol CO_2 m^{-2} s^{-1})	Leaf N (mg N g^{-1})	Leaf P (mg P g^{-1})	N:P
Acacia oblongifolia	109.8 ± 14.9	40.1 ± 3.9	17.8 ± 2.0	0.31 ± 0.10	67
Banksia attenuata	63.8 ± 11.5	38.4 ± 5.1	11.3 ± 1.4	0.31 ± 0.6	39
B. serrata	129.2 ± 23.5	35.9 ± 5.9	6.5 ± 0.5	0.25 ± 0.03	27
Eucalyptus dunnii	163.5 ± 6.1	32.7 ± 5.8	19.2 ± 1.1	1.18 ± 0.04	16
E. fastigata	204.6 ± 12.6	33.2 ± 5.7	18.0 ± 0.5	1.50 ± 0.28	13
E. saligna	144.7 ± 3.5	34.3 ± 8.0	21.3 ± 1.2	1.35 ± 0.39	19
E. tereticornis	100.7 ± 18.0	39.1 ± 5.0	16.3 ± 0.7	0.78 ± 0.09	21
E. todtiana	118.4 ± 10.3	27.0 ± 7.3	11.8 ± 1.1	0.38 ± 0.05	32
Liquidambar styraciflua	138.4 ± 22.3	20.0 ± 8.0	17.7 ± 1.4	1.83 ± 0.42	11
Persoonia levis	100.1 ± 13.9	12.7 ± 3.5	7.8 ± 0.3	0.30 ± 0.04	24

Figure S1. Time series of measurements of A_{net} before, during and after a pulse of low pO_2 was delivered to the leaf chamber for two *Eucalyptus* species (a, b). At the flow rate used, 65 sec was the time constant for mixing. Data shown are examples from (a) *Eucalyptus todtiana* measured at Lesueur National Park in Western Australia, and (b) *E. tereticornis* measures at EucFACE in NSW, Australia, for measurements at a C_a of 40 Pa. The final measurement in low pO_2 before switching O_2 back to normal pO_2 was considered at equibilibrium and was used in the calculations.

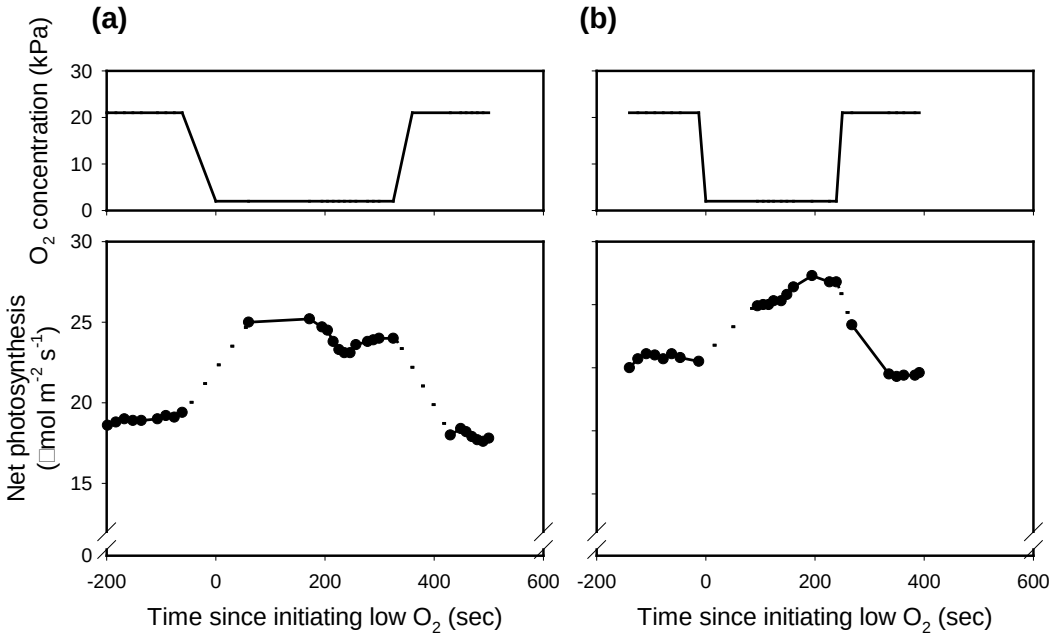

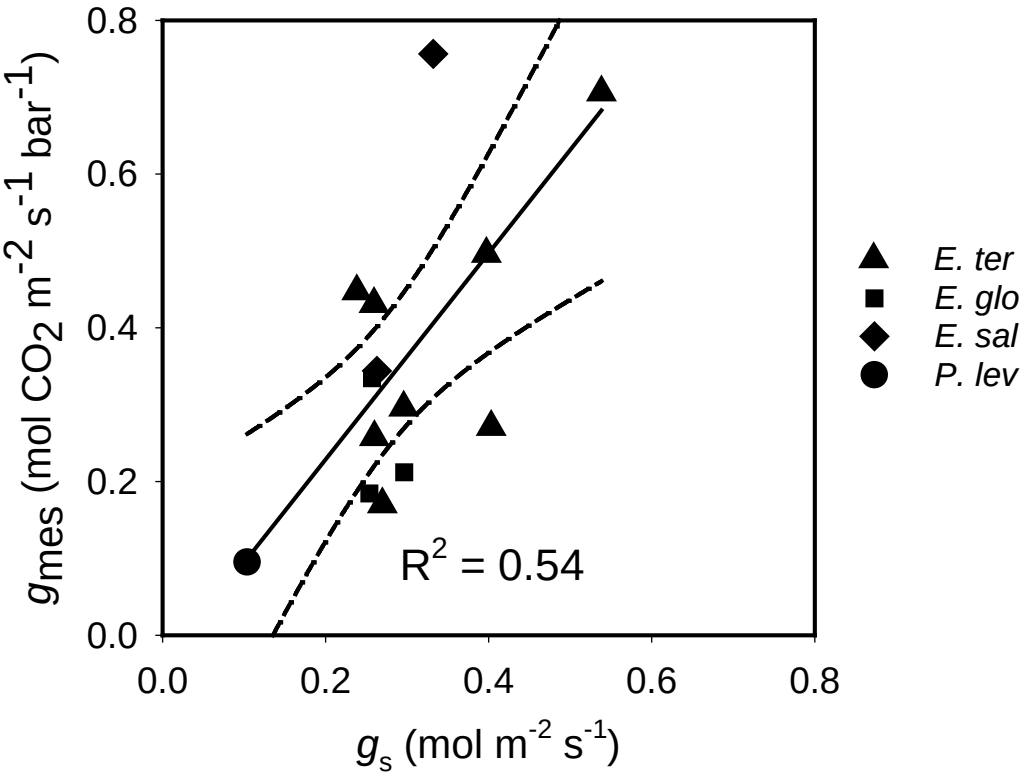
0.8
0.6
0.4
0.2
0.0
0.0
0.2
0.4
0.6
0.8
g_{mes} (mol CO_2 m^{-2} s^{-1} bar^{-1})
g_s (mol m^{-2} s^{-1})
R^2 = 0.54
E. ter
E. glo
E. sal
P. lev